

AD-A048 357

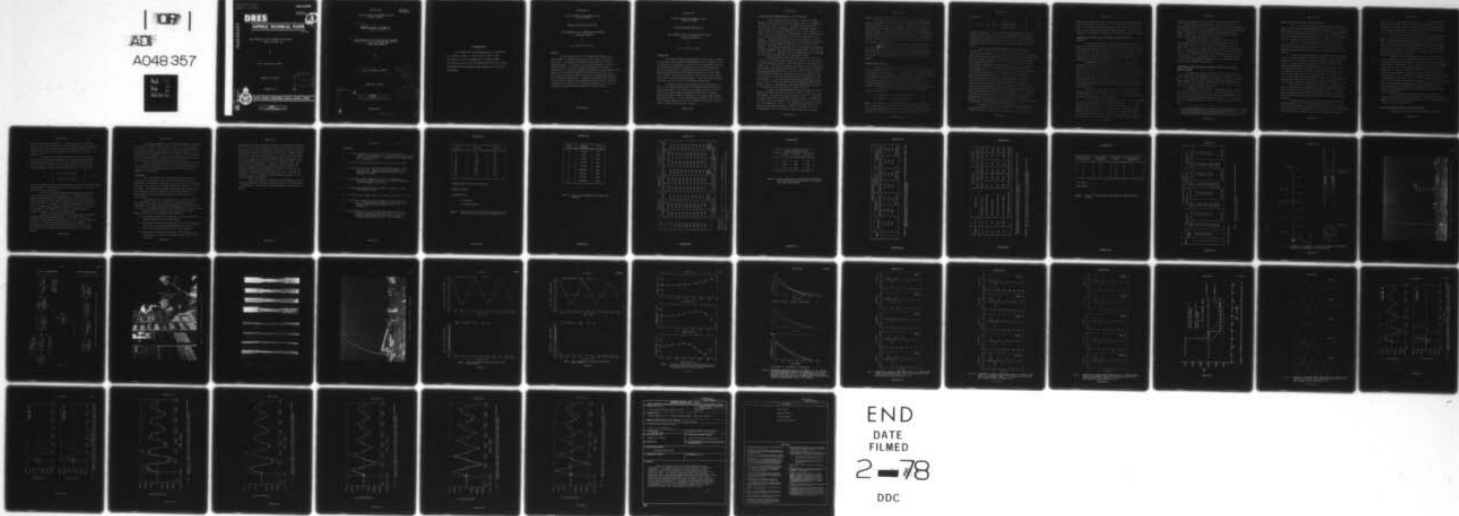
DEFENCE RESEARCH ESTABLISHMENT SUFFIELD RALSTON (ALBERTA) F/G 15/6
BLAST RESPONSE OF 35 FT FIBREGLASS WHIP ANTENNA - EVENT DICE TH--ETC(U)
NOV 77 G V PRICE, C G COFFEY

UNCLASSIFIED

DRES-TECHNICAL PAPER-448

NL

TOP
AD
A048 357



END
DATE
FILED
2-78
DDC

3
S/N

AD A 048357

DRES

SUFFIELD TECHNICAL PAPER

NO. 448

BLAST RESPONSE OF 35 FT FIBREGLASS WHIP ANTENNA
- EVENT DICE THROW (U)

by

G.V. Price and C.G. Coffey

PROJECT NO. 97-80-01

November 1977

DDC
PACIFIC
JAN 12 1978
REF ID: A 123456789
D

12-11-1

DDC FILE COPY



DEFENCE RESEARCH ESTABLISHMENT SUFFIELD : RALSTON : ALBERTA

WARNING

The use of this information is permitted subject to recognition
of proprietary and patent rights".

UNCLASSIFIED

UNLIMITED
DISTRIBUTION

DEFENCE RESEARCH ESTABLISHMENT SUFFIELD
RALSTON ALBERTA

14

DRES -

SUFFIELD TECHNICAL PAPER ~~NO~~ 448

6

BLAST RESPONSE OF 35 FT FIBREGLASS WHIP ANTENNA

- EVENT DICE THROW (1)

by

10

G.V. Price and C.G. Coffey

11

Nov 77

12

48P.

PROJECT NO. 97-80-01

ACCESSION NO.	
RTIS	White Section <input checked="" type="checkbox"/>
DDG	Black Section <input type="checkbox"/>
WARNING	<input type="checkbox"/>
JUSTIFICATION	<input type="checkbox"/>
BY	
DISTRIBUTION/AVAILABILITY CODE	
ORIG.	AVAIL. AND OR SPECIAL
A	

WARNING
The use of this information is permitted subject to recognition
of proprietary and patent rights.

UNCLASSIFIED

D D C
RECORDED
JAN 12 1978
RECORDED
D

403 104

mt

ACKNOWLEDGEMENT

The authors wish to acknowledge Messrs. F.H. Winfield, R.L. Campbell, W. Ngo, J.J. Vesso, and R.N. Moss for their contributions in field instrumentation of the Whip Antenna. Contributions by the staff of the Experimental Model Shop, the DRES Photography Group and the DRES Computer Group are also gratefully acknowledged.

UNCLASSIFIED

DEFENCE RESEARCH ESTABLISHMENT SUFFIELD
RALSTON ALBERTA

SUFFIELD TECHNICAL PAPER NO. 448

BLAST RESPONSE OF 35 FT FIBREGLASS WHIP ANTENNA
- EVENT DICE THROW (U)

by

G.V. Price and C.G. Coffey

ABSTRACT

The blast response of 35 ft fibreglass Whip Antennas was investigated in a free-field blast trial and in numerical simulation experiments. The antennas satisfactorily withstood the air blast loading at nominal 7.0, 10.0 and 12.2 psi peak overpressure locations in Event Dice Throw. The numerical model predictions for the natural frequencies are in excellent agreement with results obtained experimentally, however the corresponding predictions for the transient strain using drag coefficients based on previous trials were approximately double the values obtained experimentally. Subsequent revised numerical predictions for the transient strains using experimental drag coefficients obtained independently in the blast trial itself have produced results in more reasonable agreement with the experimental transient strains.

(U)

UNCLASSIFIED

UNCLASSIFIED

DEFENCE RESEARCH ESTABLISHMENT SUFFIELD
RALSTON ALBERTA

SUFFIELD TECHNICAL PAPER NO. 448

BLAST RESPONSE OF 35 FT FIBREGLASS WHIP ANTENNA
- EVENT DICE THROW (U)

by

G.V. Price and C.G. Coffey

INTRODUCTION

The Defence Research Establishment Suffield (DRES), in support of the Canadian Forces (Maritime) requirement on blast hardening of ships and components, has conducted a series of tests to determine the ability of certain antenna designs to withstand various blast overpressures. During Event Dice Throw, a 620-ton AN/F0 free-field blast trial conducted by the United States Defense Nuclear Agency at the White Sands Missile Range in New Mexico on October 6, 1976, several antenna designs were tested at various overpressure levels. One of the antenna designs evaluated in the trial was a 35 ft fibreglass Whip Antenna.

The objectives of this study were to determine the ability of three 35 ft fibreglass Whip Antennas to withstand the effects of blast waves at the nominal 7.0, 10.0 and 12.2 psi peak overpressure levels respectively, and to compare the measured response of the antennas against theoretical predictions determined by a computer model recently developed at DRES [1]. It was intended that experimental verification of the computer model would lead to a criterion for predicting the blast response of whip antenna designs in general.

UNCLASSIFIED

INSTALLATION AND INSTRUMENTATION OF THE WHIP ANTENNAS

The Whip Antenna design evaluated in the study was Model AS5085-SR manufactured by Valcom Ltd., Guelph, Ontario. A schematic of the antenna is shown in Figure 1. According to the manufacturer [2], the main shaft of the antenna was composed of alternate fibreglass layers at 90° and 0° angles relative to the axis of the antenna. The volume ratio of longitudinal to circumferential fibres was approximately 2:1 throughout the antenna except in the region of the base of the antenna. The lower three feet of the shaft was increased in size by additional circumferential wrappings up to 3/4 in thick (the additional wrappings at the base added no additional flexural strength to the antenna). The antenna was fabricated in two pieces which joined together through an embedded brass coupling located approximately 18 ft from the base (see Figure 1). Additional physical characteristics of the antenna, as supplied by the manufacturer, are presented in Table 1.

Three Whip Antennas were installed for the Event Dice Throw field trial. The antennas were located at the nominal 7.0, 10.0 and 12.2 psi peak overpressure locations (1135, 940 and 875 ft respectively from ground zero). For discussion purposes, the antennas will be referred to by the nominal peak overpressure locations at which they were installed. Each antenna was mounted on a 24 in x 30 in x 21.5 in steel box (DRES drawing MES-CDT-100-C3-2) of a type used in a previous multi-ton field trial (Event Dial Pack, held at DRES in 1970) as a mounting for a GRP Whip Antenna [3]. The steel box assemblies were subsequently bolted to 5 ft x 8 ft x 2 ft heavy reinforced concrete foundations (DRES drawing MES-CDT-100-C3-1). A photograph of the three Whip Antennas installed for the Event Dice Throw field trial is shown in Figure 2.

Five pairs of MICRO-MEASUREMENTS type EA-41-10CBE-120 strain gauges were bonded directly to the outer surface of the nominal 7.0 psi Whip Antenna. The gauge locations are shown in Figure 1. In addition, two strain gauge pairs were bonded to the outer surface of the nominal 10.0 and 12.2 psi Whip Antennas. The locations of the nine strain gauge pairs are summarized in Table 2. The gauges which constitute a strain gauge pair were bonded to opposite sides of the antennas on a line corresponding to the blast direction, thereby measuring the maximum

flexural strain at the specified cross-sections.

The signals from the strain gauge pairs were conditioned with bridge and balance units, amplified, F.M. multiplexed and then recorded on 14-track magnetic tape with a frequency response of DC to 4 KHz. In this fashion, five channels of experimental data were multiplexed onto one tape channel, a procedure which was required by the large number of DRES data channels and limited number of tape recorders. A block diagram describing the instrumentation is shown in Figure 3, and a photograph of the DRES Instrumentation Bunker in which the data signals were processed and recorded is shown in Figure 4.

In addition to the strain gauge data, the response of the 7.0, 10.0 and 12.2~~0~~psi Whip Antennas was recorded respectively on a LOCAM high-speed camera at 500 frames per second, a FASTAIR high-speed camera at 320 frames per second and a FASTAIR high-speed camera at 600 frames per second. A time mark generator was used to confirm the above film speeds.

COMPUTER MODEL SIMULATION

A numerical procedure was developed at DRES to predict the elastic response of a variable cross-section cantilever beam when subjected to a transient air blast load [1]. The procedure begins with the Bernoulli-Euler equation of a vibrating beam. The normal modes and natural frequencies of the beam are determined by solving the differential equations for free vibration using successive relaxation, Rayleigh quotient and Gram-Schmidt orthogonalization numerical techniques. The forced vibration solution is obtained using normal mode coordinates and Laplace transforms.

The computer model simulation used a clamped-free boundary condition of the form

- (a) clamp at $x=0$, zero displacement and slope,
- (b) free at $x=L$, zero moment and shear,

} (1)

where x is a distance coordinate measured from the base of the antenna and L is the length of the antenna. In addition, the following values for the drag coefficient C_D were used in computing the aerodynamic drag portion of the blast wave loading on the antenna in the first set of

simulations:

$$CD = \left\{ \begin{array}{ll} 0.7, & M \geq 0.48, Re \geq 3 \times 10^5, \\ 0.6, & M < 0.48, Re \geq 3 \times 10^5, \\ 1.2, & M < 0.48, Re < 3 \times 10^5. \end{array} \right\} \quad (2)$$

In the above equation, M is the instantaneous Mach number of the flow incident on the antenna, and Re is the instantaneous Reynolds number (based on local diameter). A revised set of drag coefficients (based on independent drag experiments in Event Dice Throw itself) were used in a subsequent simulation experiment, to be considered in detail in a later section.

The structure of the Whip Antenna was represented in the computer model in such a way as to simulate the mass and projected (normal to blast direction) cross-sectional area profiles of the antenna. Three different mass/projected cross-sectional area profiles were considered. The first profile (simulation A) corresponded to physical data supplied by the manufacturer (Table 1; [2]). The second profile (simulation B) corresponded to antenna wall thicknesses measured from x-ray examination of the nominal 7.0 psi Whip Antenna (radiography examination by R.M. Hardy and Associates [4]). The final profile (simulation C) corresponded to micrometer measurements of test samples cut out of the antenna to determine the wall thicknesses for the nominal 7.0 psi Whip Antenna. With these measurements adjustment to the profiles near the base and in the vicinity of the junction between lower and upper portions of the antenna were made to account for the additional mass (measured) and stiffening in the indicated regions. In addition, the third simulation used a mass-weighted average value for Young's Modulus based on tensile tests performed by R.M. Hardy and Associates (Figure 5; [5]). In summary, simulations A and B were based on antenna features which were known or measured prior to the blast trial, while simulation C was based on antenna properties which were obtained in destructive tests and measurements of the nominal 7.0 psi Whip Antenna following the blast trial.

A comparison of the three simulations for the mass/projected cross-sectional area profiles of the nominal 7.0 psi Whip Antenna is presented in Table 3. Simulation A (manufacturer's data) is found to

differ significantly from simulations B and C (measured data) above the lower 3 ft portion of the antenna. The differences in the profiles will result in differences in the corresponding strain predictions, a point which will be examined in more detail under the heading, "Comparison of Theoretical and Experimental Bending Strain Histories: Event Dice Throw".

COMPARISON OF THEORETICAL AND EXPERIMENTAL NATURAL FREQUENCIES:
TWANG TEST

Prior to the blast trial, a "Twang Test" was performed to obtain free vibration strain data for the Whip Antennas. A static load was applied near the top of each antenna using an anchored nylon rope at a pull angle of 30⁰ to the horizontal. The load was subsequently released electrically and the strain data for free vibration was recorded. The experiment was performed to determine the natural frequencies of the antennas and to verify the test instrumentation.

A photograph of the Twang Test apparatus is shown in Figure 6. The apparatus consisted of a 1/4 in nylon rope attached to a bracket at the 30 ft location on each of the antennas and anchored to a truck, a 6000 lb capacity L.A.B. Corp. Quick Release Hook, a hand-operated mechanical winch to take up slack in the system, and a Transducers Inc. strain-type load cell (model ML2-151-1K) with a Budd Strain indicator readout (model P-350) to measure the applied load. The applied loads were monitored locally with the load cell while the bending strains as measured by the strain gauges bonded to the antenna were recorded remotely in the Instrumentation Bunker.

The loads on the antennas were released electrically and the bending strain data for free vibration ("Twang Test") were recorded in the Instrumentation Bunker. In this fashion it was possible to establish that the test instrumentation was operational.

A Fourier analysis was subsequently performed for the experimental strain data to determine the natural frequencies of each antenna. The free vibration strain history and corresponding Fourier analysis for gauges 2 and 5 are presented in Figures 7 and 8. As shown, the lowest natural frequency for the 7.0 psi Whip Antenna is sharply identified as 1.27 cps by the Fourier analysis, while the higher natural frequencies are less distinct. The best resolution of the higher natural frequencies

occurs for the gauge located in the upper region of the antenna, gauge 5. The three lowest natural frequencies of the three antennas, as determined from a Fourier analysis of the Twang Test strain measurements, are presented in Table 4. The observed differences between the experimental natural frequencies of the three antennas are due to differences in antenna construction. In particular, the 10.0 and 12.2 psi antennas were 15 inches longer than the 7.0 psi antenna [6].

The theoretical (numerical simulation) predictions for the three lowest natural frequencies and corresponding normal modes for simulation A of the 7.0 psi Whip Antenna are presented in Figure 9. Normal modes of a similar general shape were obtained for simulations B and C. A comparison of the natural frequencies for simulations A, B and C of the 7.0 psi Whip Antenna against the experimental values obtained from the Twang Test is presented in Table 5. It is apparent from this comparison that the predicted frequencies are in excellent agreement with the values obtained experimentally.

COMPARISON OF THEORETICAL AND EXPERIMENTAL BENDING STRAIN HISTORIES:
EVENT DICE THROW

The numerical simulation model was used to generate bending strain predictions corresponding to two types of Friedlander overpressure waves. The two sets of overpressures respectively correspond to Defense Nuclear Agency (DNA) pre-trial predictions (blast data A) and average measured¹ blast wave properties (blast data B) at the nominal 7.0, 10.0 and 12.2 psi peak over pressure locations.

A comparison of the two sets of Friedlander overpressure waves is presented in Table 6 and Figure 10. It should be noted that despite the lower peak overpressure in the experimental Friedlander waves, the total impulse associated with the experimental waves is 18 to 49% higher than the corresponding impulse of the 7.0, 10.0 and 12.2 psi predicted waves.

¹ The free-field overpressure at the base of the three antennas was measured using ten Bytrex Model HFH-100 strain-type pressure transducers [7]. The "measured" overpressure wave properties were considered to be the average of the properties determined by the individual pressure transducers.

PREDICTIONS BASED ON PRE-TRIAL DRAG COEFFICIENTS

Three sets of bending strain predictions were calculated using the pre-trial drag coefficients summarized in equation (2). The discussion which follows considers only the predictions for the 7.0 psi Whip Antenna, since the trends apparent in this set of results are representative of the results obtained with the other antennas. A summary of the essential features of the three prediction experiments is presented in Table 7.

The first set of predictions (predictions 1) used physical data supplied by the contractor (simulation A) together with pre-trial blast data provided by DNA (blast data A). This set of predictions is therefore based on pre-trial physical and blast data supplied by external agencies.

A comparison of predicted against experimental strain histories for the 7.0 psi Whip Antenna is presented in Figure 11, and an evaluation of the ability of the model to predict peak bending strains is given in Table 8. Although certain gauge locations display reasonably good agreement between predicted and experimental strains, at most locations the measured strains are considerably smaller than predicted. This is apparent from the large value for the average ratio of peak theoretical to experimental strains (1.62; see Table 8). In addition, the ratio of peak theoretical to experimental strains fluctuates considerably from gauge to gauge, indicating that the mass profile simulation does not accurately follow the mass distribution trends in the antenna itself.

The second set of predictions (predictions 2) used physical data corresponding to x-ray measurements at DRES (simulation B) together with pre-trial blast data provided by DNA (blast data A). As in the previous prediction experiment, this calculation is based on pre-trial data since non-destructive techniques were used to determine the antenna properties.

A comparison of the corresponding predicted strains against the experimental results is provided in Figure 12 and Table 8. It is noted that the predictions are in poorer agreement with the experimental results than in the first prediction set, a result which was not anticipated since more accurate simulation data was used to describe the antenna

structure in this case compared to the former. It is therefore apparent that the earlier prediction set 1 involved compensating errors in that an erroneous simulated mass profile produced errors which compensated for an unknown factor which is causing the strain predictions to be much larger than the experimental values would indicate.

The third set of predictions (predictions 3) used experimentally determined physical and blast data as input to the numerical prediction model. This represents the best available input data to the numerical prediction model, and should therefore produce the best strain predictions. The mass profile in the calculation corresponds to measurements obtained from post-trial destructive tests performed on the 7.0 psi Whip Antenna (simulation C), and the air blast data corresponds to average measured blast wave properties (blast data B).

A comparison of the corresponding predicted strains against the experimental results is presented in Figure 13 and Table 8. Similar to the previous prediction experiments, the predictions are considerably larger than the experimental results. However, the ratio of peak theoretical to experimental strains fluctuates considerably less from gauge to gauge compared to the earlier predictions, indicating that the mass profile simulation more accurately follows the actual mass distribution trends in the antenna itself. In addition, it should be noted that this prediction is based on blast data which has an 18 to 49% larger positive phase impulse than in the earlier prediction experiments. The earlier prediction sets 1 and 2 therefore had compensating errors, since artificially low pre-trial DNA blast data compensated for an unknown factor which is causing the strain predictions to be much larger than the experimental values would indicate.

At this point, the only remaining area to be evaluated in assessing the cause of the poor performance of the numerical prediction model lies with the empirical drag coefficients. This will be considered in detail in the following section.

PREDICTIONS BASED ON DICE THROW DRAG COEFFICIENTS

An aerodynamic drag project was independently undertaken in

the Event Dice Throw field trial [8]. The drag forces on cylinders of various diameters were determined using free-flight measurement techniques, and preliminary drag coefficient results, as shown in Figure 14, are now available in the low Reynolds number regime, applicable to the Whip Antenna study.

It is apparent from these preliminary results that the drag coefficients at low Reynolds number in Event Dice Throw are much smaller than anticipated from earlier field trials. Based on the preliminary results presented in Figure 14, a drag coefficient profile appropriate to the low Reynolds number regime in Event Dice Throw is of the form

$$C_D = \begin{cases} 0.3, & M < 0.48, Re \geq 4 \times 10^5, \\ 0.6, & M < 0.48, Re < 4 \times 10^5. \end{cases} \quad (3)$$

It should be noted that this profile is based on preliminary drag measurements, and the reader is referred to the final drag study report [8] for more details and revised C_D profiles.

A final set of strain predictions was produced using the drag coefficient profile specified by equation (3). The predictions were computed using experimentally determined physical and blast data (mass profile simulation C, blast data B) as input to the numerical prediction model (see Table 7). A comparison of the corresponding predicted strains against the experimental results is presented in Figures, 15, 16, and 17, and Table 8. The comparisons for the 7.0 psi Whip Antenna are repeated in Figures 18 to 22 in an enlarged format.

In general, the predicted strains are found to be in reasonable agreement with the experimental strains. The average ratio of peak theoretical to experimental bending strains is 1.27, a value significantly less than the results from the previous prediction experiments. The best agreement between the predicted and experimental strains occurs with gauges 4 and 5, located in the upper portion of the 7.0 psi Whip Antenna.

The poorest agreement in this prediction experiment is obtained for gauge 6, located in the lower portion of the 10.0 psi Whip Antenna (see Figures 1 and 16). This result is in part a consequence of using a mass profile simulation based on the 7.0 psi antenna (simulation C) in generating the time response of the 10.0 psi antenna. As noted earlier, the three antennas differ in construction [6], and measured mass profile data was not available for the 10.0 and 12.2 psi antennas.

Due to strain gauge failure early in the pressure/time history of the blast wave, experimental verification of strain predictions from three of the four strain gauge pairs on the 10.0 and 12.2 psi Whip Antennas is not available.

CONCLUSIONS

The blast response of 35 ft fibreglass Whip Antennas was investigated in a free-field blast trial and in numerical simulation experiments. The antennas satisfactorily withstood the air blast loading at nominal 7.0, 10.0 and 12.2 psi peak overpressure locations in Event Dice Throw. The corresponding antenna response was modelled numerically, and predictions of natural frequencies and transient bending strains were generated for various antenna mass profile simulations and air blast loadings.

The predicted natural frequencies were in excellent agreement with experimental results and the transient strain predictions using experimental drag coefficients obtained independently in the blast trial itself were in reasonable agreement with the experimental transient strains.

Accuracy of the transient strain predictions was found to depend significantly on the following three conditions:

- (a) the computer simulation must make use of the mass profile and physical properties of the actual antenna;
- (b) the computer simulation must make use of the air blast properties of the actual blast wave (peak overpressure, positive phase duration, and particularly the positive phase impulse);
- (c) the computer simulation must make use of the aerodynamic drag coefficient (C_D) relevant to the antenna geometry and blast wave in question.

Conditions (a) and (b) are generally known with some degree of certainty prior to a blast trial (if necessary, destructive material tests may be carried out on a duplicate antenna to establish the correct mass profile and physical properties for the numerical simulation). However, there appears to be some doubt regarding correct drag coefficient relationship for air blast waves (as function of Reynolds number, Mach number, and blast wave properties) particularly in the low Reynolds number regime which applies to whip antennas. Evidence of drag coefficient uncertainty was apparent in this study through the large differences in transient strain predictions obtained using pre-trial C_D profiles and profiles of C_D determined from the blast trial itself. Reducing the uncertainty in C_D at low Reynolds and Mach numbers represents an area requiring further investigation.

Subject to an accurate simulation of the antenna mass profile, blast wave properties, and drag coefficient profiles, the computer model is recommended as a design tool in the development of whip antennas in general.

REFERENCES

1. G.V. Price, "Numerical Simulation of the Air Blast Response of Tapered Cantilever Beams (U)". Defence Research Establishment Suffield, Ralston, Alberta. Suffield Technical Paper No. 447. 1977. UNCLASSIFIED.
2. S.B. Clarke, Private Communication to G.V. Price, April 23, 1976.
3. L.W. Tamke and B.R. Long, "Evaluation of GRP Whip Antenna - Event Dial Pack (U)". Event Dial Pack Symposium Report, Vol. 1. Defence Research Board of Canada, pp. 263-274. 1973. FOR OFFICIAL USE ONLY.
4. R.D. Vergetti, Private Communication to G.V. Price Regarding a Radiographic Inspection on April 21, 1976 by D.R. Shannon. File No. CXR76-824. May 4, 1976.
5. R.M. Hardy and Associates Metal Test Report, Lab Order No. 6103-1795, December 8, 1976.
6. G.V. Price, Private Communication to R. McInnis, DMCS-6, May 27, 1976.
7. F.H. Winfield, "Event Dice Throw - Canadian Air Blast Measurements (U)". Defence Research Establishment Suffield, Ralston, Alberta. Suffield Technical Paper No. 451. 1977. UNCLASSIFIED.
8. A.W.M. Gibb and D.A. Hill, "Free-Flight Measurement of the Drag Forces On Cylinders in Event Dice Throw (U)". Defence Research Establishment Suffield, Ralston, Alberta. Suffield Technical Paper No. 453. 1977. UNCLASSIFIED.

UNCLASSIFIED

x^1 (ft)	OD ² (in)	ID ³ (in)
2	6.5	4.4
6	5.0	4.1
10	4.5	3.7
14	4.15	3.4
18	3.9	3.0
22	3.0	2.6
26	2.4	2.1
20	2.1	1.8
34	1.9	1.5

¹ Distance from the base of the antenna.

² Outside diameter.

³ Inside diameter.

$$E = 3.9 \times 10^6 \text{ psi}$$

$$\rho = 0.002298 \text{ slugs/in}^3$$

Table 1: Physical features of the Valcom AS5085-SR fibreglass Whip Antenna, as supplied by the manufacturer [2].

UNCLASSIFIED

UNCLASSIFIED

Gauge	Antenna (nominal)	x (ft)
1	7.0 psi	3.5
2	7.0 psi	10.5
3	7.0 psi	17.0
4	7.0 psi	18.4
5	7.0 psi	24.0
6	10.0 psi	10.5
7	10.0 psi	24.0
8	12.2 psi	10.5
9	12.2 psi	24.0

Table 2: Strain gauge locations of the three Whip
Antennas.

UNCLASSIFIED

UNCLASSIFIED

x (in)	Simulation A			Simulation B			Simulation C		
	ID (in)	OD (in)	Wt (lb)	ID (in)	OD (in)	Wt (lb)	ID (in)	OD (in)	Wt (lb)
0.0	4.400 ¹	6.500 ¹	48.41	5.537 ¹	6.457 ¹	22.63	5.540 ¹	9.640 ²	84.54
41.9	4.283	5.942	30.03	4.411	5.199	15.89	4.167	4.965	15.90
83.7	4.002	4.878	17.30	3.845	4.503	11.73	3.845	4.535	12.15
125.6	3.665	4.459	14.74	3.678	4.205	9.93	3.640	4.177	10.04
167.4	3.403	4.154	14.37	3.381	3.929	8.96	3.341	3.901	12.81
209.2	3.056	3.935	11.33	3.224	3.709	6.67	2.551 ²	3.609	10.72
251.1	2.707	3.241	5.90	2.619	2.997	4.37	2.659	3.067	4.65
292.9	2.298	2.638	3.57	2.280	2.582	3.22	2.251	2.562	3.54
334.8	1.957	2.257	3.05	2.047	2.319	2.49	2.021	2.346	2.91
376.6	1.695	2.030	1.851	2.071		1.825	2.075		2.06
418.5	1.500 ¹	1.900 ¹	3.17	1.777 ¹	1.947 ¹	1.82	1.741 ¹	1.937 ¹	
			Total: 151.87			Total: 87.71			Total: 159.32
	$E = 3.9 \times 10^6 \text{ psi} [2]$	$E = 3.9 \times 10^6 \text{ psi} [2]$		$E = 4.27 \times 10^6 \text{ psi} [5]$	$E = 4.27 \times 10^6 \text{ psi} [5]$				
	$\rho = 0.002298 \text{ slugs/in}^3$	$\Delta x = 41.8 \text{ in}$	$N = 10$	$L = 418.5 \text{ (34.88 ft)}$					

UNCLASSIFIED

¹ Extrapolated.
² Calculated based on the measured mass distribution; calculation depends on Δx .

Table 3: Physical features of the three computer simulations of the 7.0 psi fiberglass whip antenna.

UNCLASSIFIED

Mode	Natural Frequencies (cps)		
	7.0 psi	10.0 psi	12.2 psi
1	1.27	1.03	1.02
2	4.20	3.46	3.52
3	9.50	8.25	7.75

Table 4: Natural frequencies of the three Whip Antennas as determined from a Fourier analysis of the Twang Test strain measurements.

UNCLASSIFIED

UNCLASSIFIED

Mode	Experimental	Natural Frequencies (cps)					
		Simulation A		Simulation B		Simulation C	
	Theoretical	Theo./Exp.	Theoretical	Theo./Exp.	Theoretical	Theo./Exp.	
1	1.27	1.47	1.16	1.33	1.05	1.34	1.06
2	4.20	4.09	0.97	4.08	0.97	4.06	0.97
3	9.50	9.55	1.01	9.47	1.00	10.16	1.07
			Avg. <u>1.05</u>		Avg. <u>1.01</u>		Avg. <u>1.03</u>

Table 5: Comparison of theoretical (numerical simulations A, B and C) and experimental (Twang Test) natural frequencies for the 7.0 psi Whip Antenna.

UNCLASSIFIED

UNCLASSIFIED

Symbol	Units	Description	Blast Data A			Blast Data B	
			7.0	10.0	12.2	7.0	10.0
P_A	psi	atmospheric pressure	12.58	12.58	12.58	12.42	12.42
T_A	°F	atmospheric temperature	54	54	54	48	48
P_0	psi	peak overpressure	7.0	10.0	12.2	6.6	9.9
t_d	msec	positive phase duration	242	189	172	250	231
I_D	psi/msec	positive phase impulse	600	695	750	707	863
κ^1	--	Friedlander decay constant	1.137	1.002	1.104	0.482	0.911
						1.009	1.009

¹The decay constant is computed based on the condition that the Friedlander wave is to be characterized by the specified values of P_0 , t_d and I_D .

Table 6: Air blast data corresponding to the pre-trial DNA predictions (blast data A) and the average measured blast wave properties (blast data B).

UNCLASSIFIED

UNCLASSIFIED

Transient Strains Prediction Set	Mass Profile Simulation ¹	Air Blast Data ²	Drag Coefficient Equation No.
1	A	A	2
2	B	A	2
3	C	B	2
4	C	B	3

¹ See Table 3.

² See Table 6.

Table 7: Summary of the numerical predictions for transient bending strains.

UNCLASSIFIED

UNCLASSIFIED

Gauge	Experi-mental	Peak Bending Strains (μ in/in)				Predictions 4	
		Theo- tical	Theo./Exp.	Theo- tical	Theo./Exp.	Theo- tical	Theo./Exp.
1	2009	2050	1.02	4601	2.29	5371	2.67
2	2381	3443	1.45	6300	2.65	6656	2.80
3	1335	3112	2.33	5773	4.32	3579	2.68
4	2376	3578	1.51	6263	2.64	4066	1.71
5	3713	7171	1.93	7712	2.08	7334	1.98
6	3902	5756	1.48	10574	2.71	11584	2.97
7	-- 1	12491	--	13137	--	13128	--
8	-- 1	7609	--	13748	--	17150	--
9	-- 1	16510	--	17136	--	19411	--
		Avg. 1.62		Avg. 2.78		Avg. 2.47	
						Avg. 1.27	

¹ Strain gauge failure.

Table 8: Comparison of peak theoretical and experimental bending strains (first quarter cycle only).

UNCLASSIFIED

UNCLASSIFIED

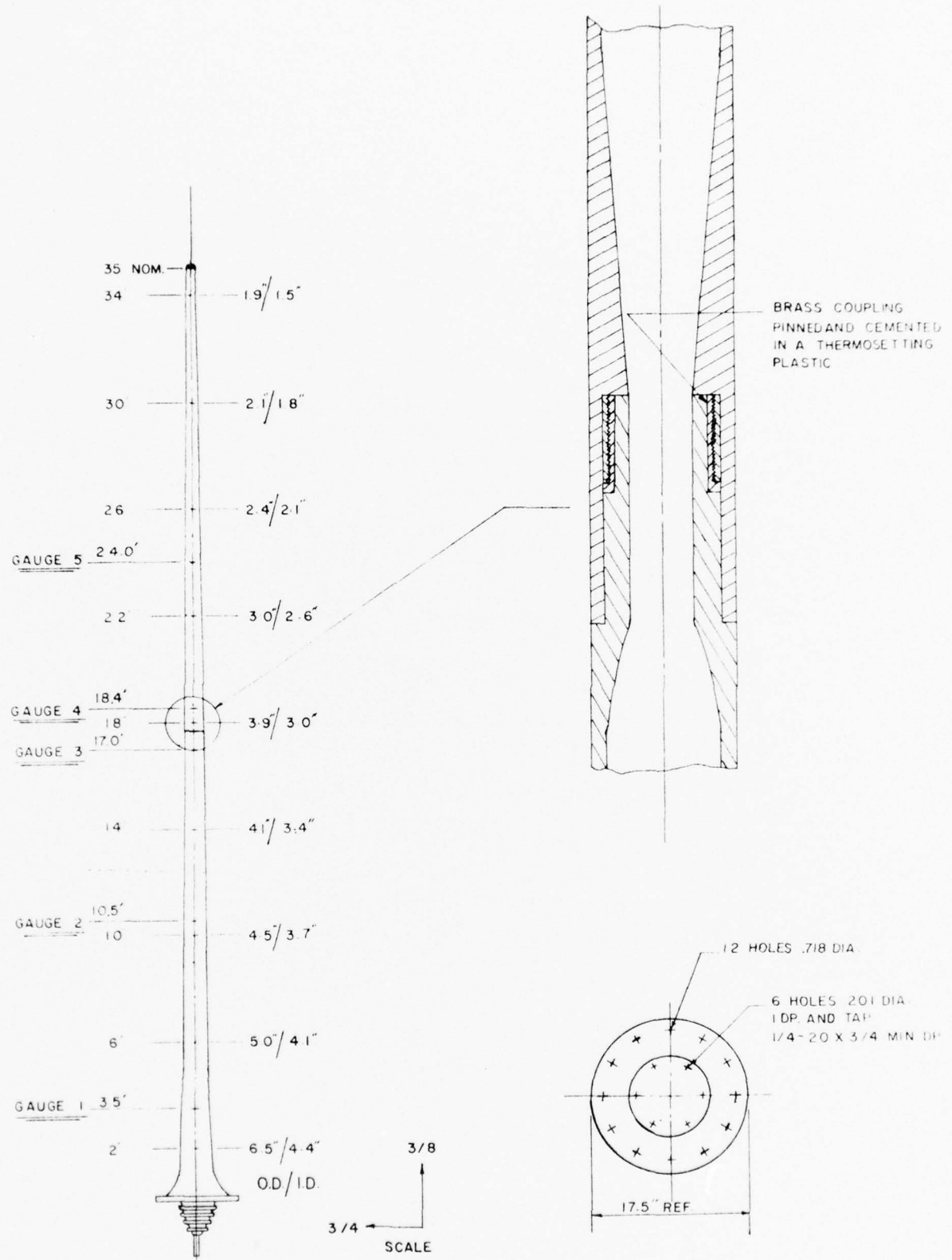


FIG. 1 SCHEMATIC OF THE NOMINAL 7.0 PSI 35 FT FIBREGLASS WHIP ANTENNA,
INCLUDING THE LOCATIONS OF THE STRAIN GAUGES

UNCLASSIFIED

UNCLASSIFIED

STP 448

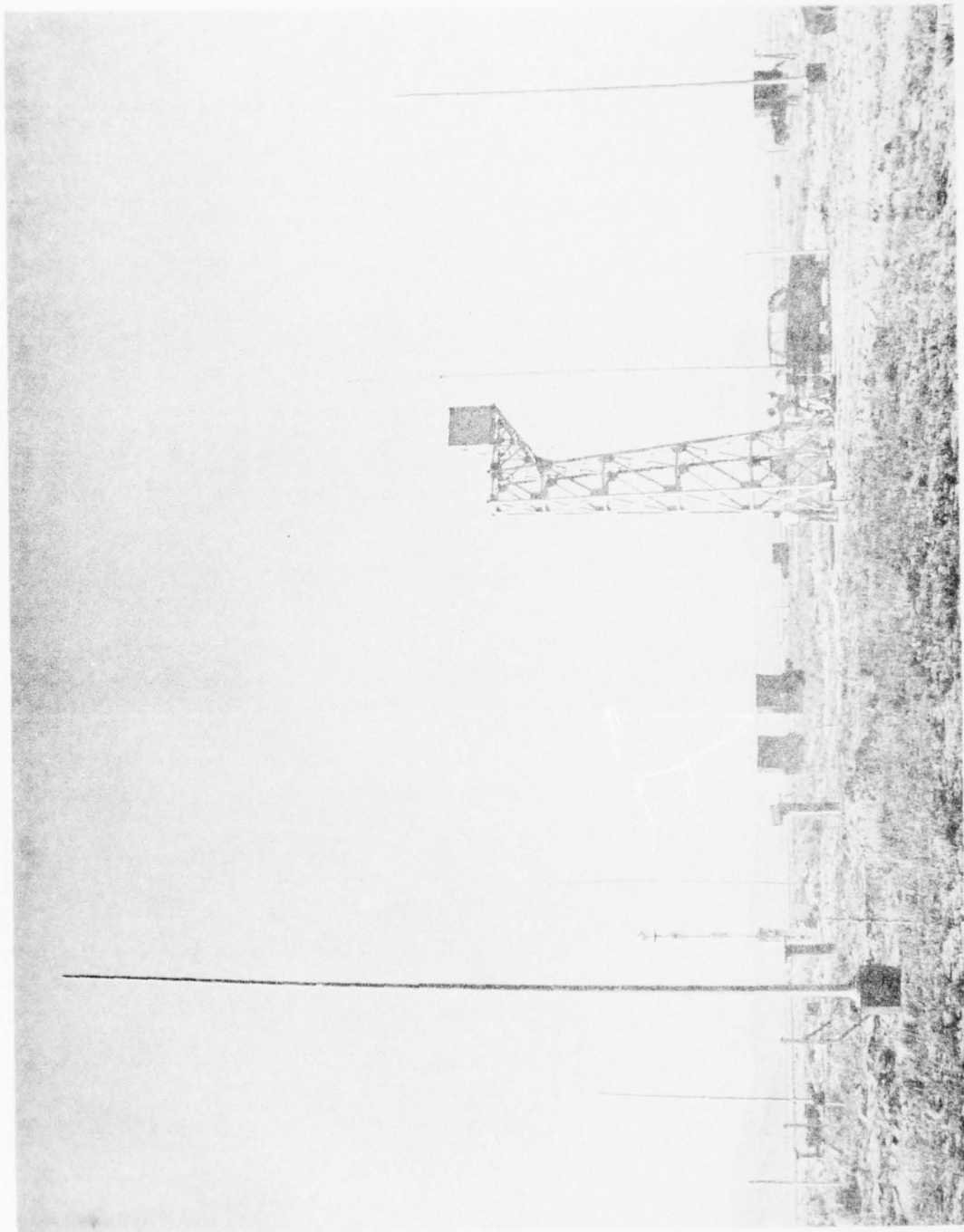


FIGURE 2: PHOTOGRAPH OF THE THREE 35 FT FIBREGLASS WHIP ANTENNAS IN EVENT DICE THROW.

UNCLASSIFIED

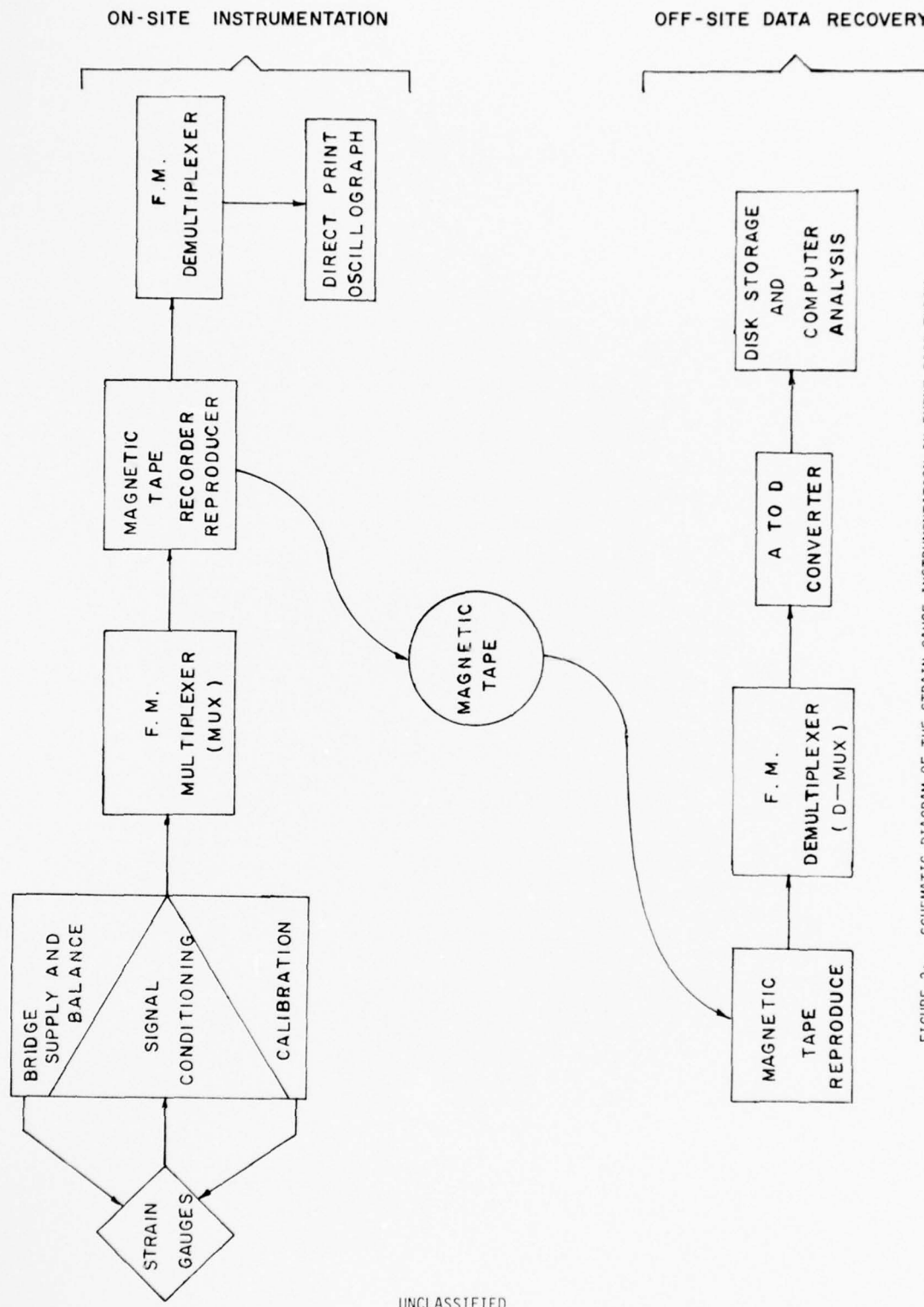
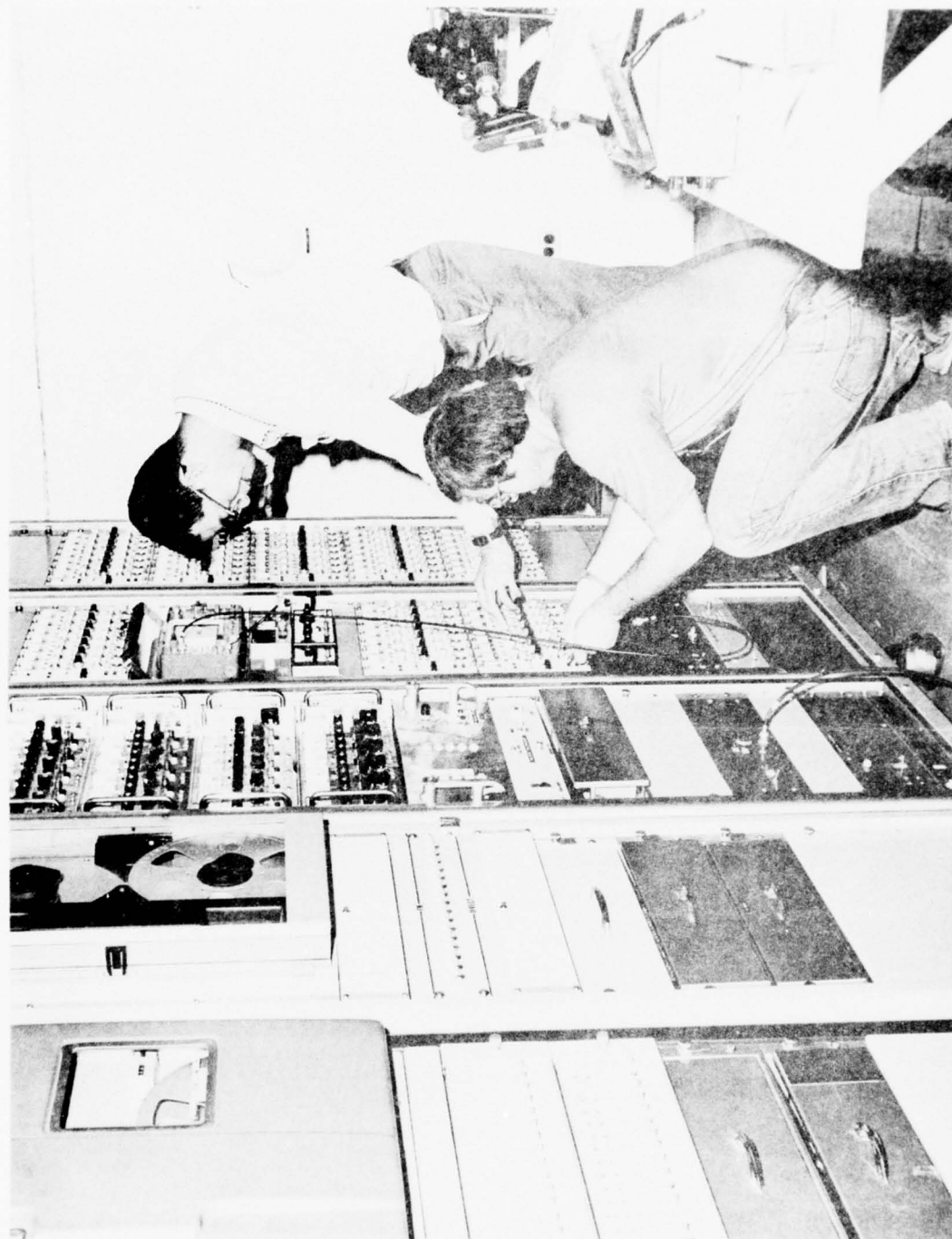


FIGURE 3: SCHEMATIC DIAGRAM OF THE STRAIN GAUGE INSTRUMENTATION IN EVENT DICE THROW.

UNCLASSIFIED

STP 448



UNCLASSIFIED

FIGURE 4: DRES INSTRUMENTATION BUNKER IN EVENT DICE THROW.

UNCLASSIFIED

STP 448

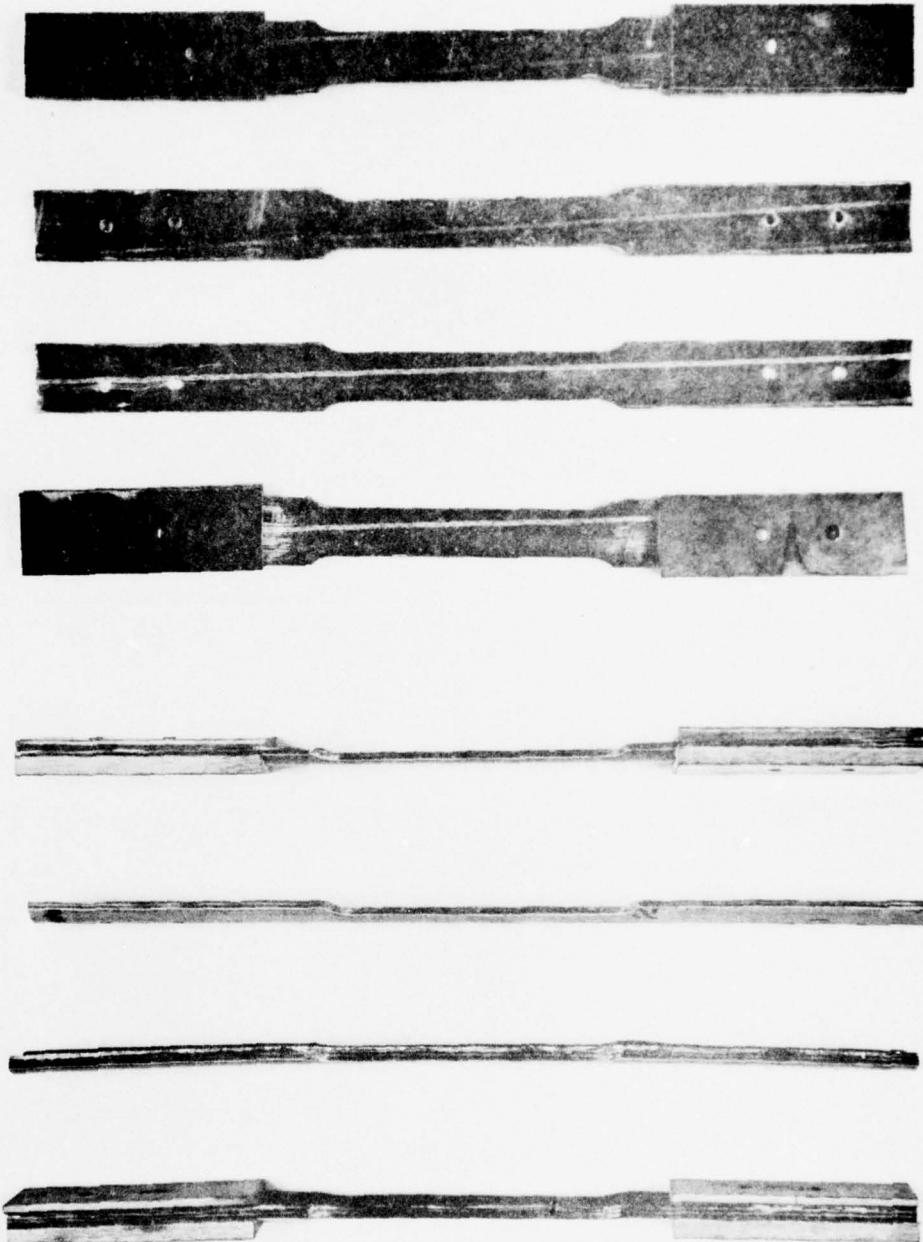
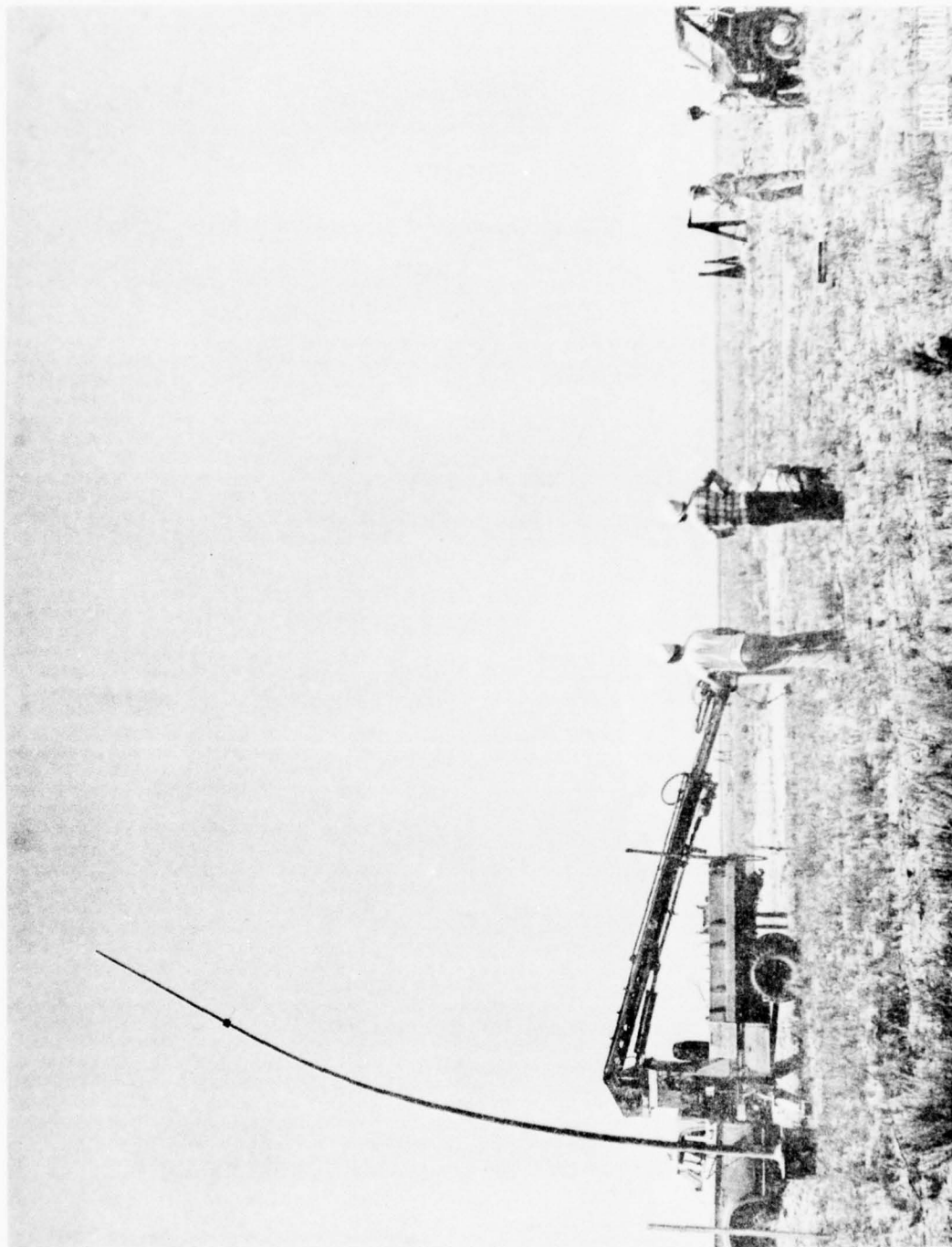


FIGURE 5: TENSILE SPECIMENS, R.M. HARDY MATERIAL TESTS [5].

UNCLASSIFIED

UNCLASSIFIED

STP 448



UNCLASSIFIED

FIGURE 6: PHOTOGRAPH OF THE TWANG TEST APPARATUS.

UNCLASSIFIED

STP 448

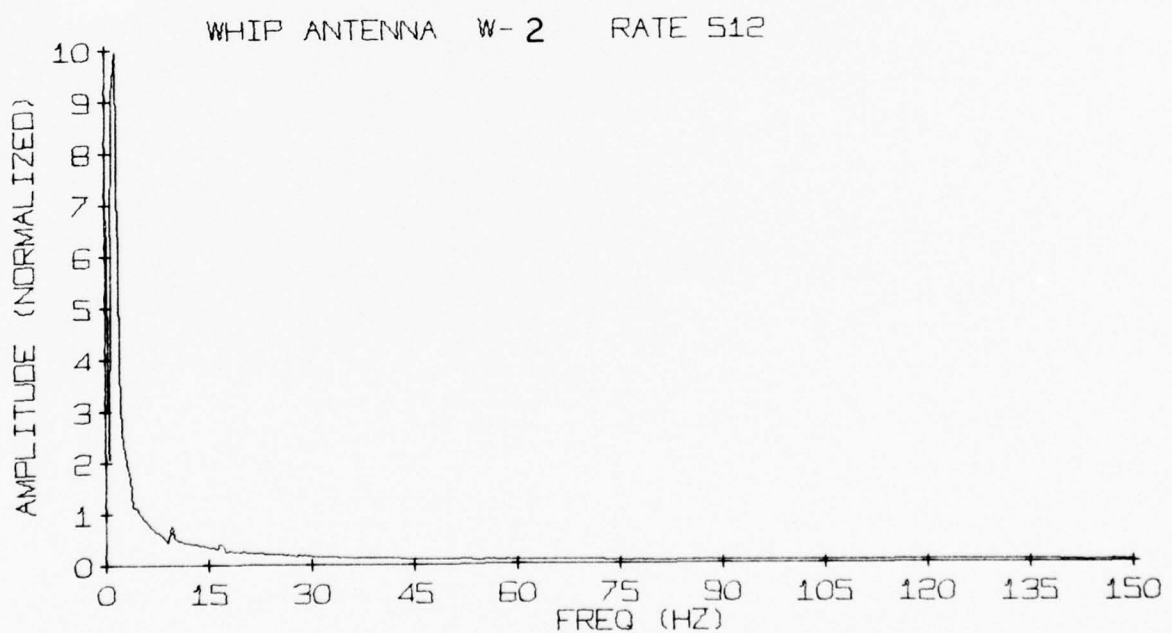
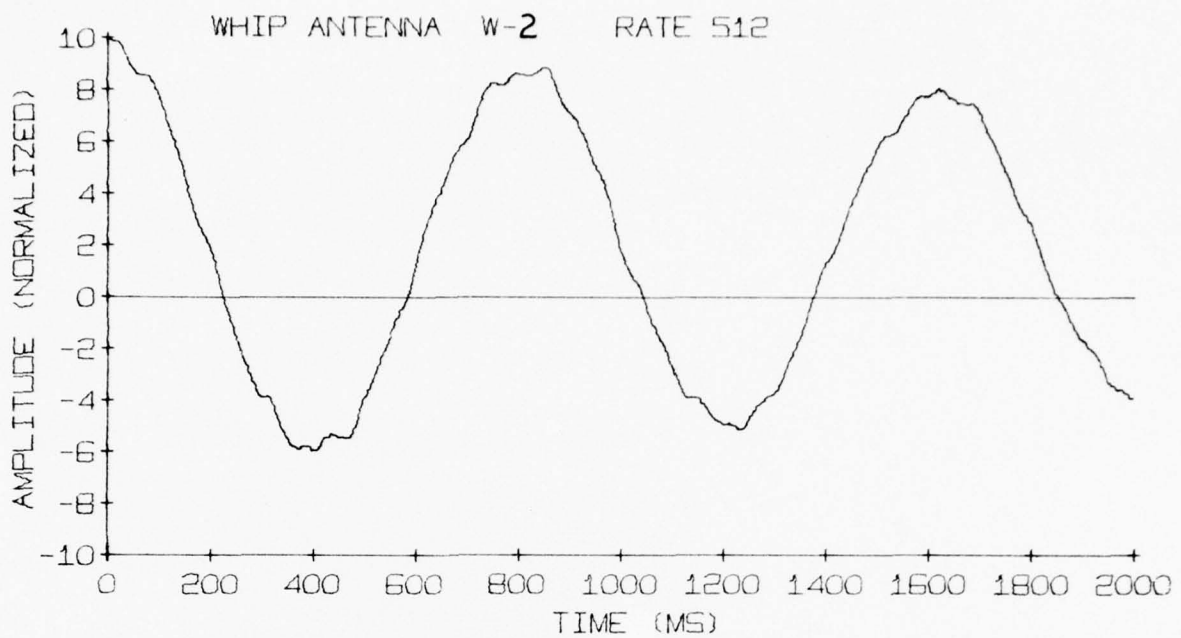


FIGURE 7: TWANG TEST BENDING STRAIN HISTORY AND CORRESPONDING FOURIER ANALYSIS FOR GAUGE 2.

UNCLASSIFIED

UNCLASSIFIED

STP 448

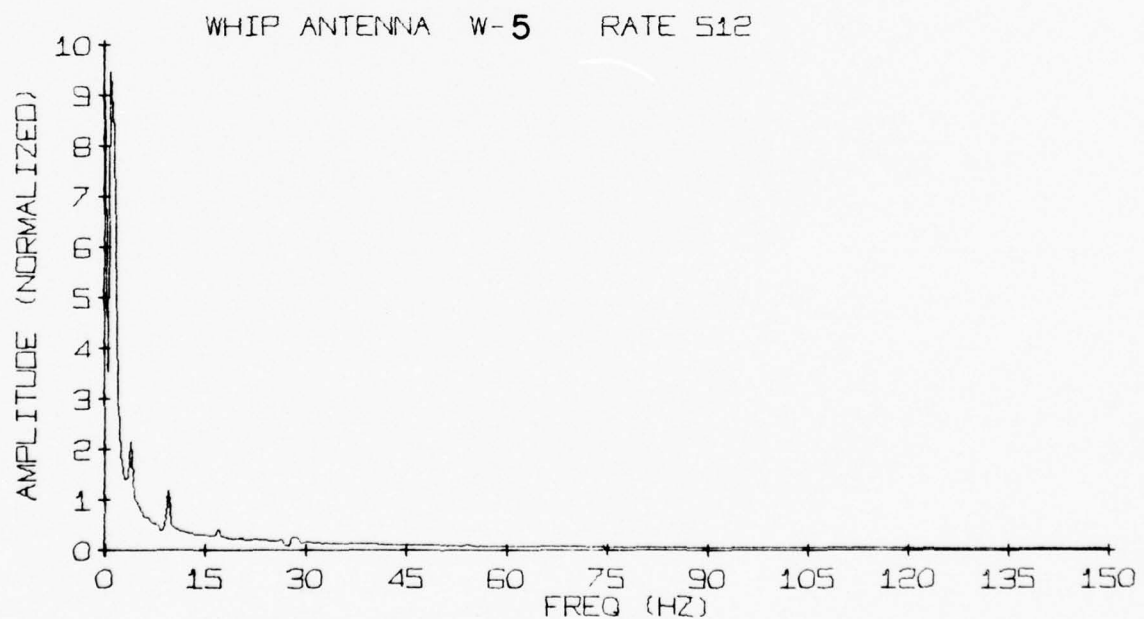
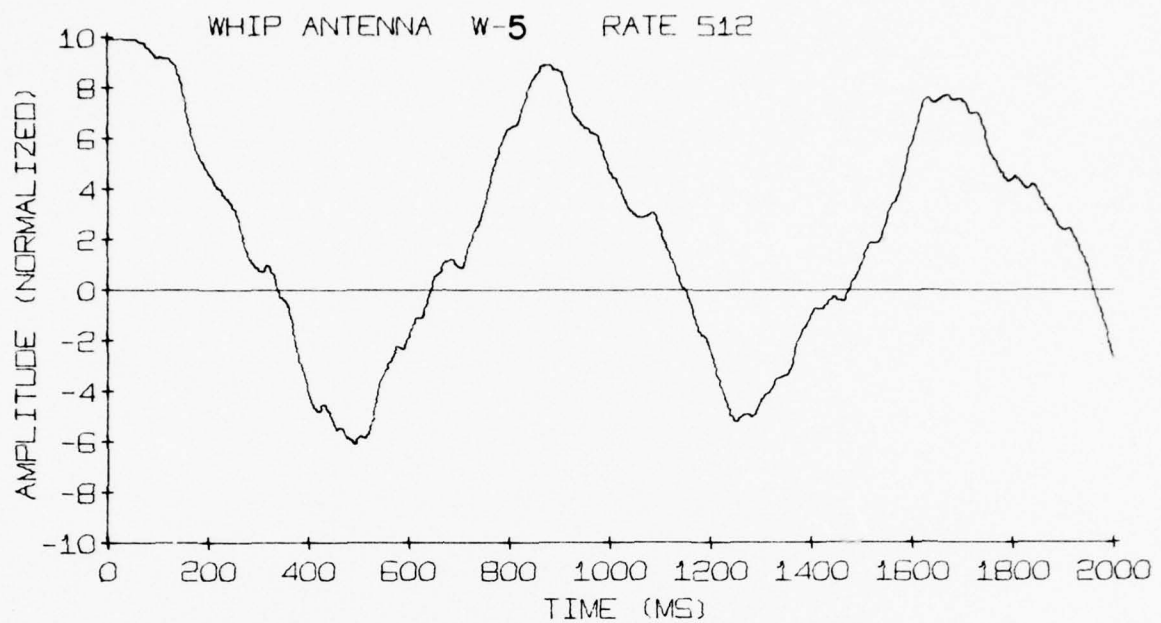


FIGURE 8: TWANG TEST BENDING STRAIN HISTORY AND CORRESPONDING FOURIER ANALYSIS FOR GAUGE 5.

UNCLASSIFIED

UNCLASSIFIED

STP 448

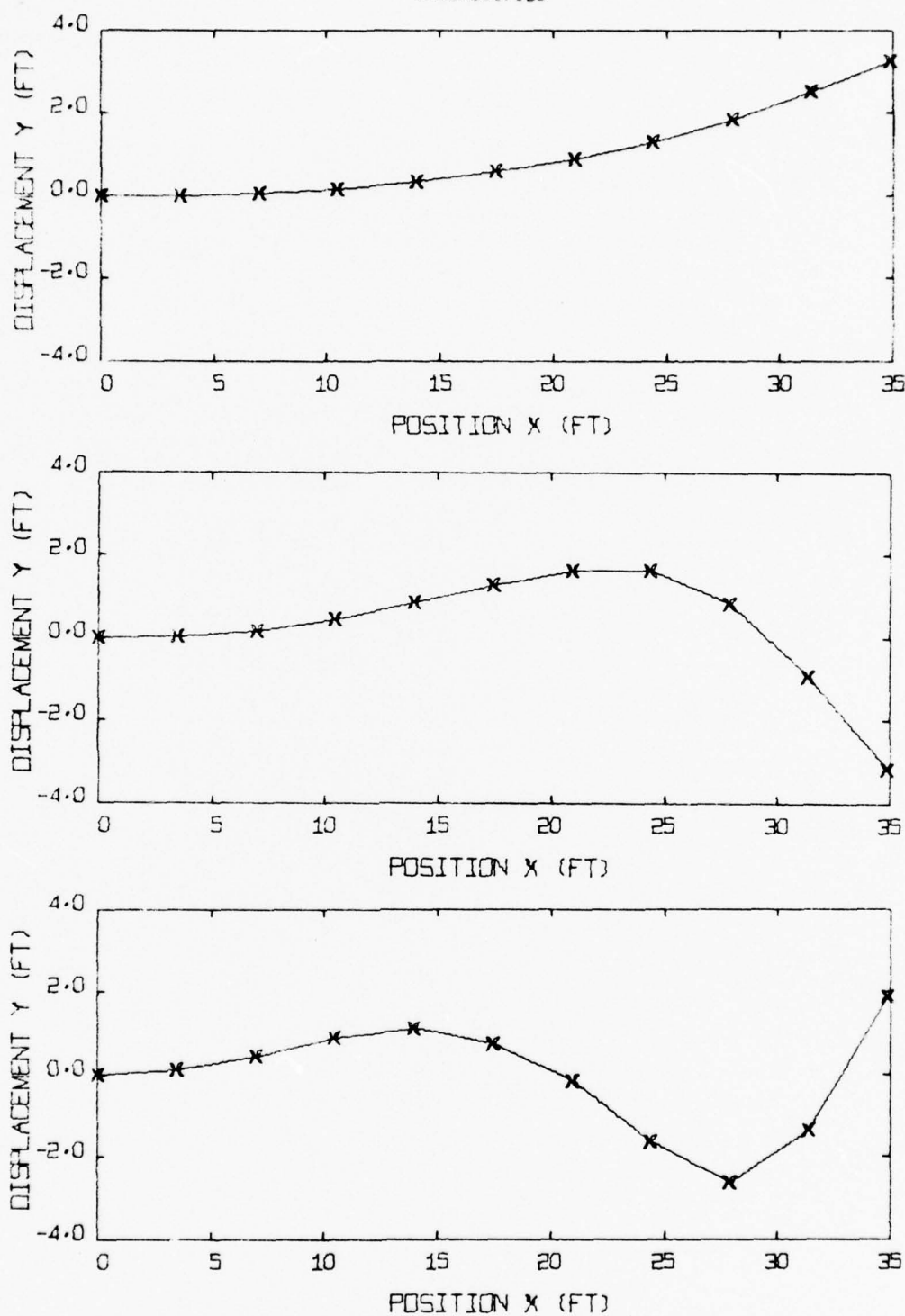
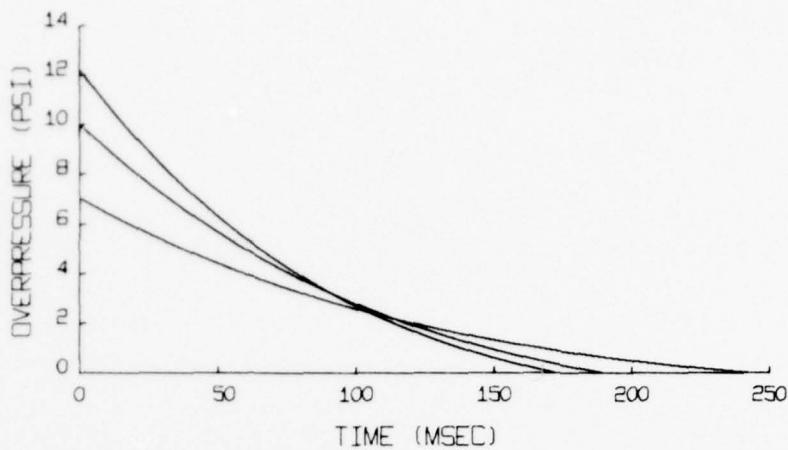
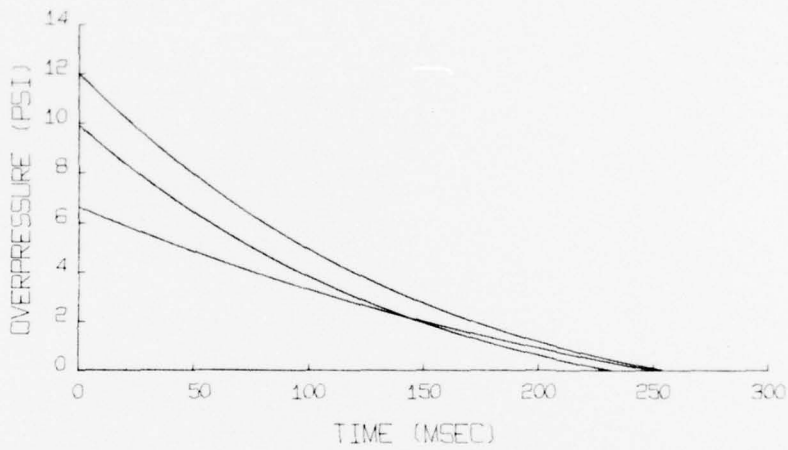


FIGURE 9: THEORETICAL (NUMERICAL SIMULATION) PREDICTIONS FOR THE THREE LOWEST NATURAL FREQUENCIES AND CORRESPONDING NORMAL MODES FOR SIMULATION A OF THE 7.0 PSI WHIP ANTENNA.

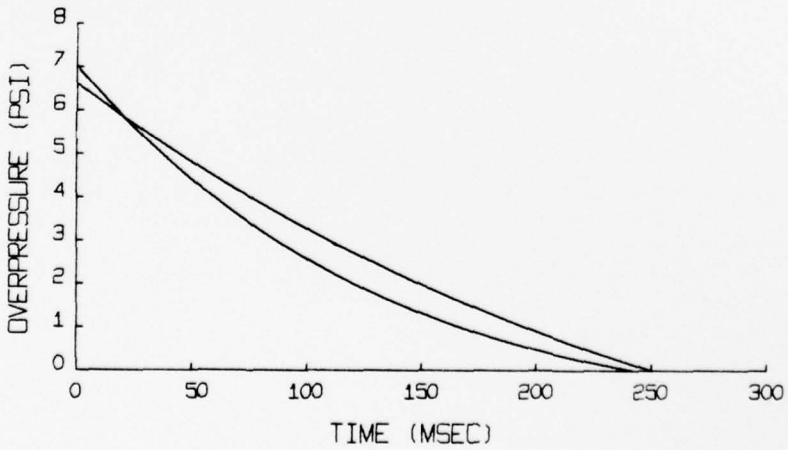
UNCLASSIFIED



(a) WHIP ANTENNA - NOMINAL OVERPRESSURE



(b) WHIP ANTENNA - EXPERIMENTAL OVERPRESSURE



(c) NOMINAL VS. EXPERIMENTAL OVERPRESSURE

FIG. 10 FRIEDLANDER OVERPRESSURE WAVES AT THE NOMINAL 7.0, 10.0, AND 12.2 PSI PEAK OVERPRESSURE LOCATIONS WHICH CORRESPOND TO (A) PRE-TRIAL DNA PREDICTIONS (BLAST DATA A), (B) AVERAGE MEASURED BLAST WAVE PROPERTIES (BLAST DATA B), AND (C) COMPARISON OF THE DNA PREDICTION AGAINST THE MEASURED WAVE AT THE 7.0 PSI LOCATION

UNCLASSIFIED

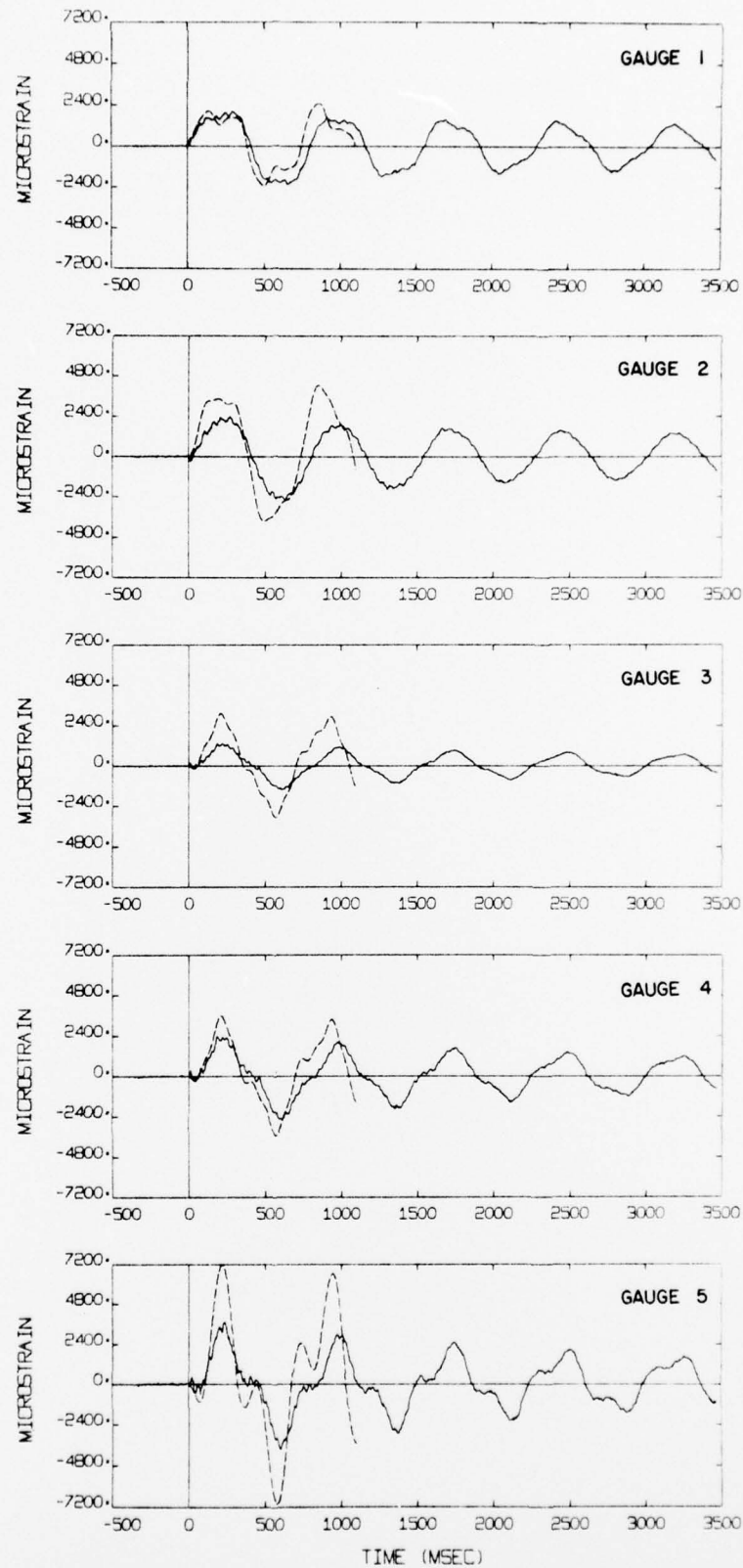


FIG. 11 COMPARISON OF BENDING STRAIN PREDICTIONS SET 1 (DASHED LINES) AGAINST THE MEASURED STRAINS (SOLID LINES) FOR THE 7.0 PSI WHIP ANTENNA AT GAUGE LOCATIONS 1 TO 5.

UNCLASSIFIED

UNCLASSIFIED

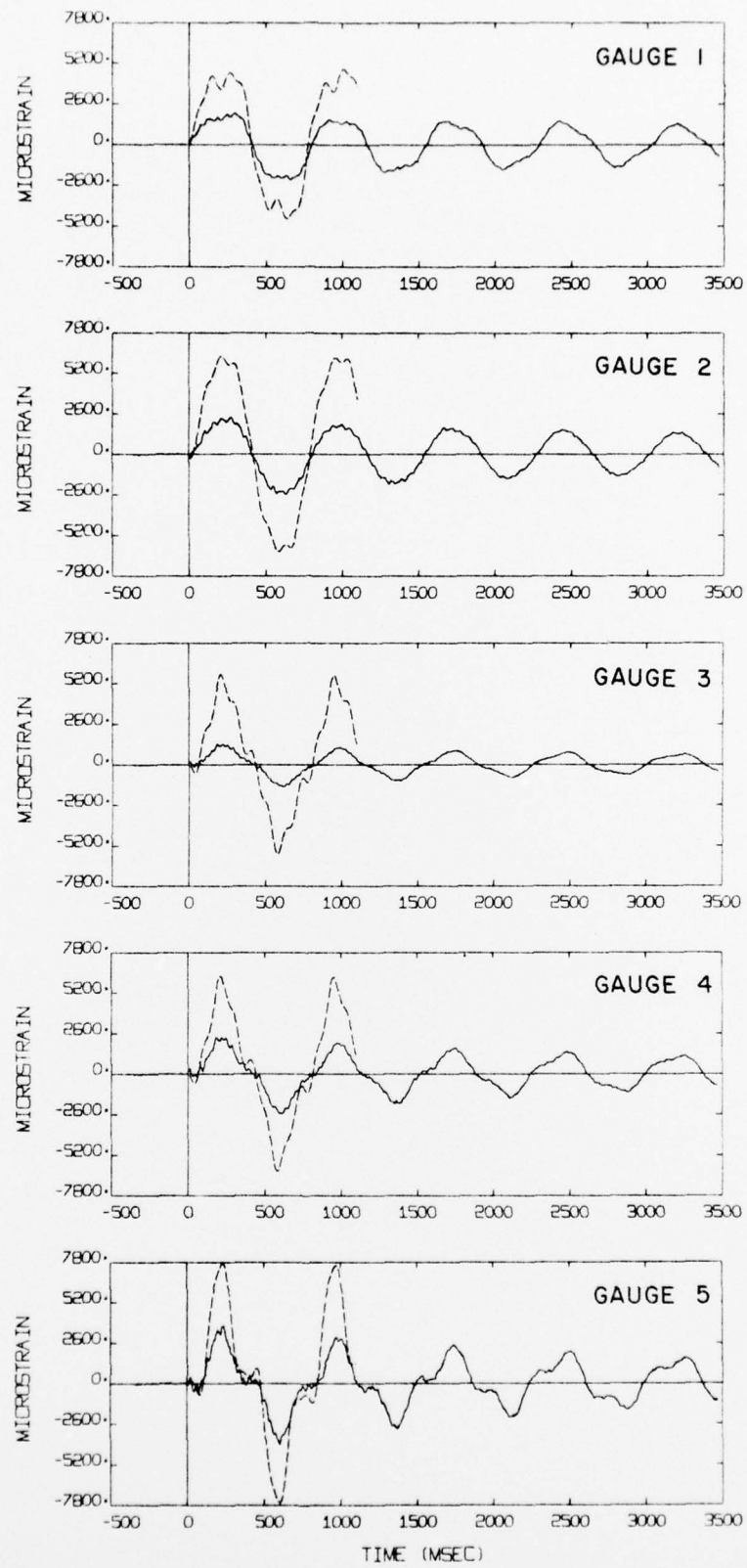


FIG. 12 COMPARISON OF BENDING STRAIN PREDICTIONS SET 2 (DASHED LINES)
AGAINST THE MEASURED STRAINS (SOLID LINES) FOR THE 7.0 PSI
WHIP ANTENNA AT GAUGE LOCATIONS 1 TO 5.

UNCLASSIFIED

UNCLASSIFIED

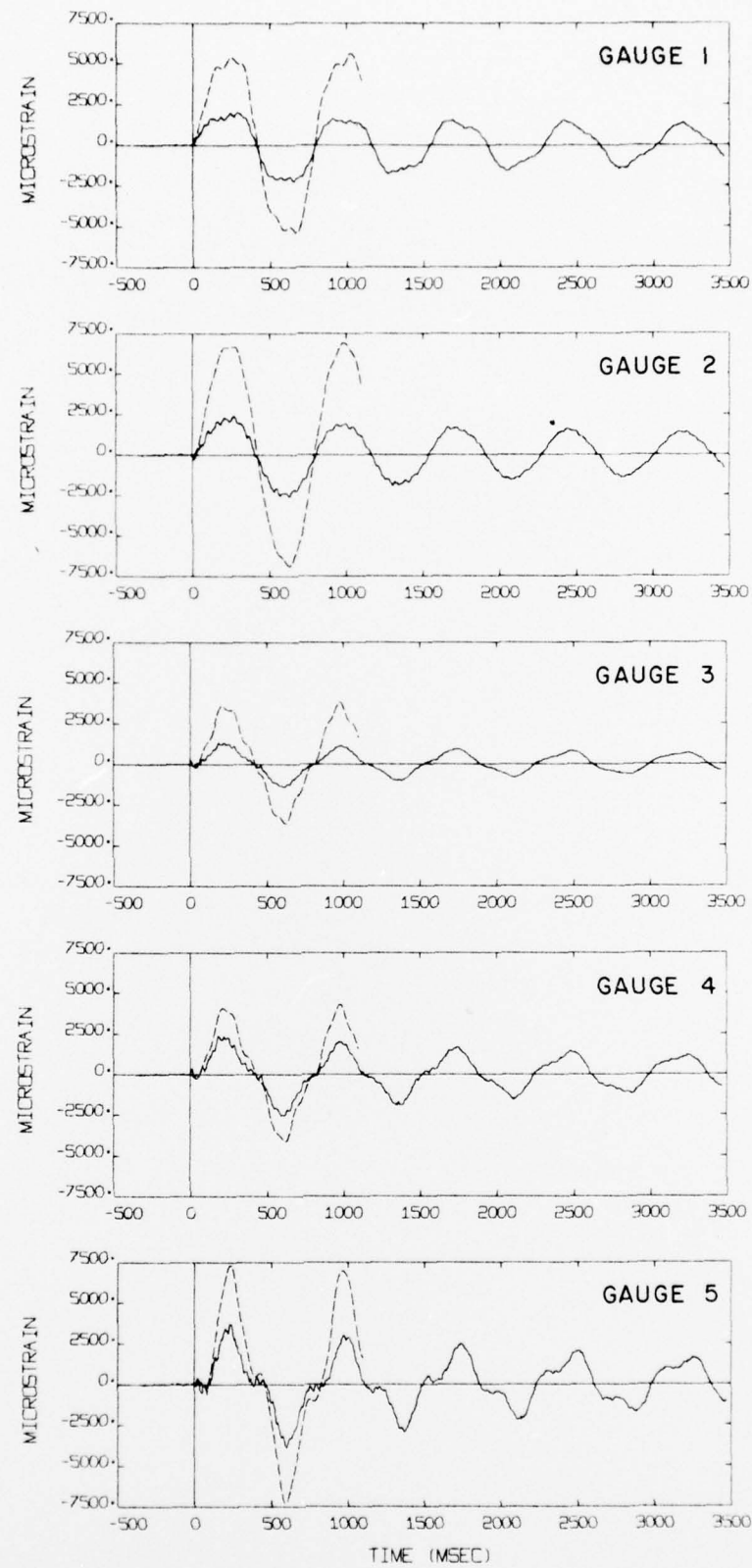
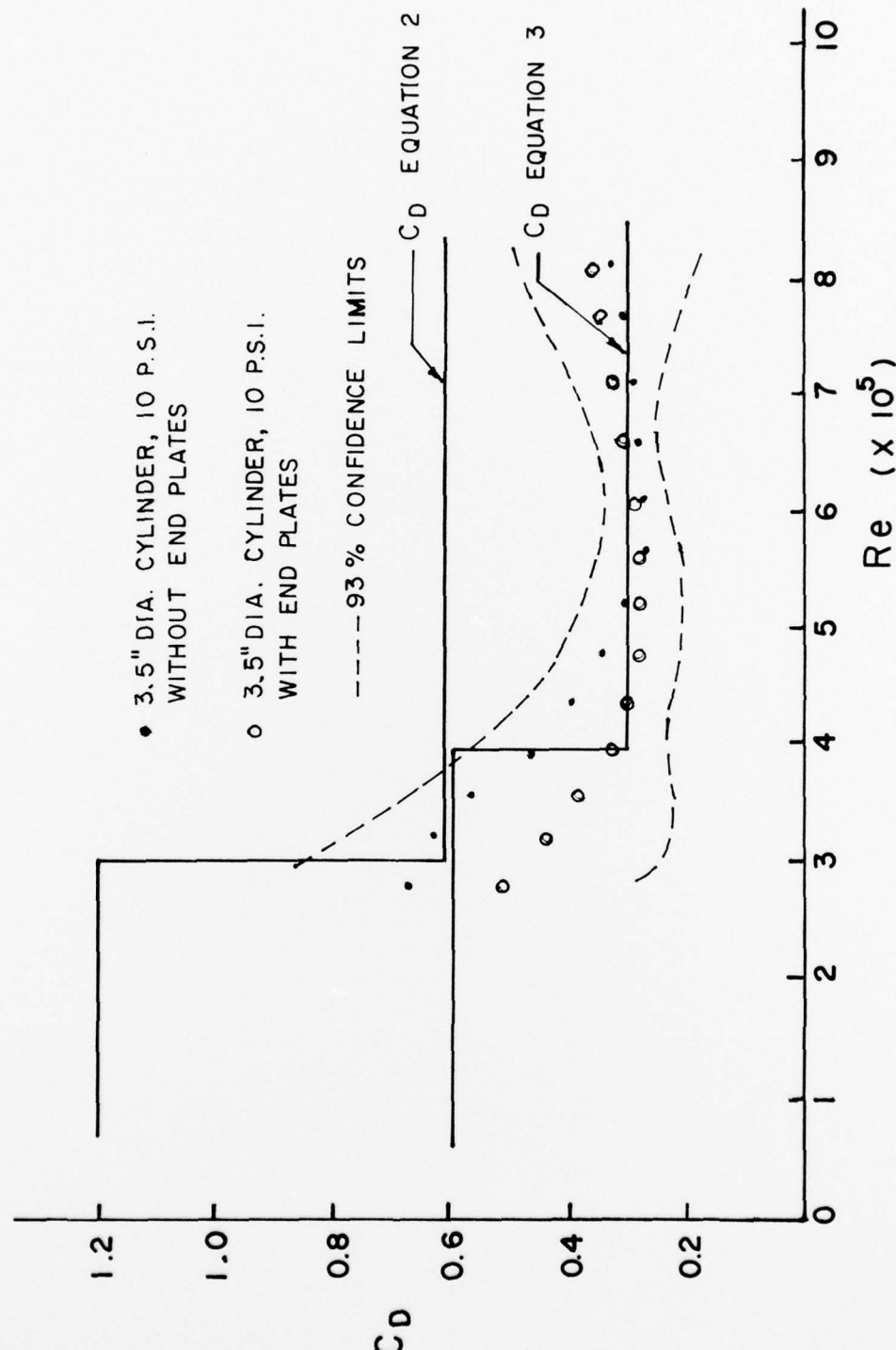


FIG. 13 COMPARISON OF BENDING STRAIN PREDICTIONS SET 3 (DASHED LINES) AGAINST THE MEASURED STRAINS (SOLID LINES) FOR THE 7.0 PSI WHIP ANTENNA AT GAUGE LOCATIONS 1 TO 5.

UNCLASSIFIED



UNCLASSIFIED

FIGURE 14: PRELIMINARY DRAG COEFFICIENT PROFILES DETERMINED FROM THE DICE THROW DRAG EXPERIMENT [8].

UNCLASSIFIED

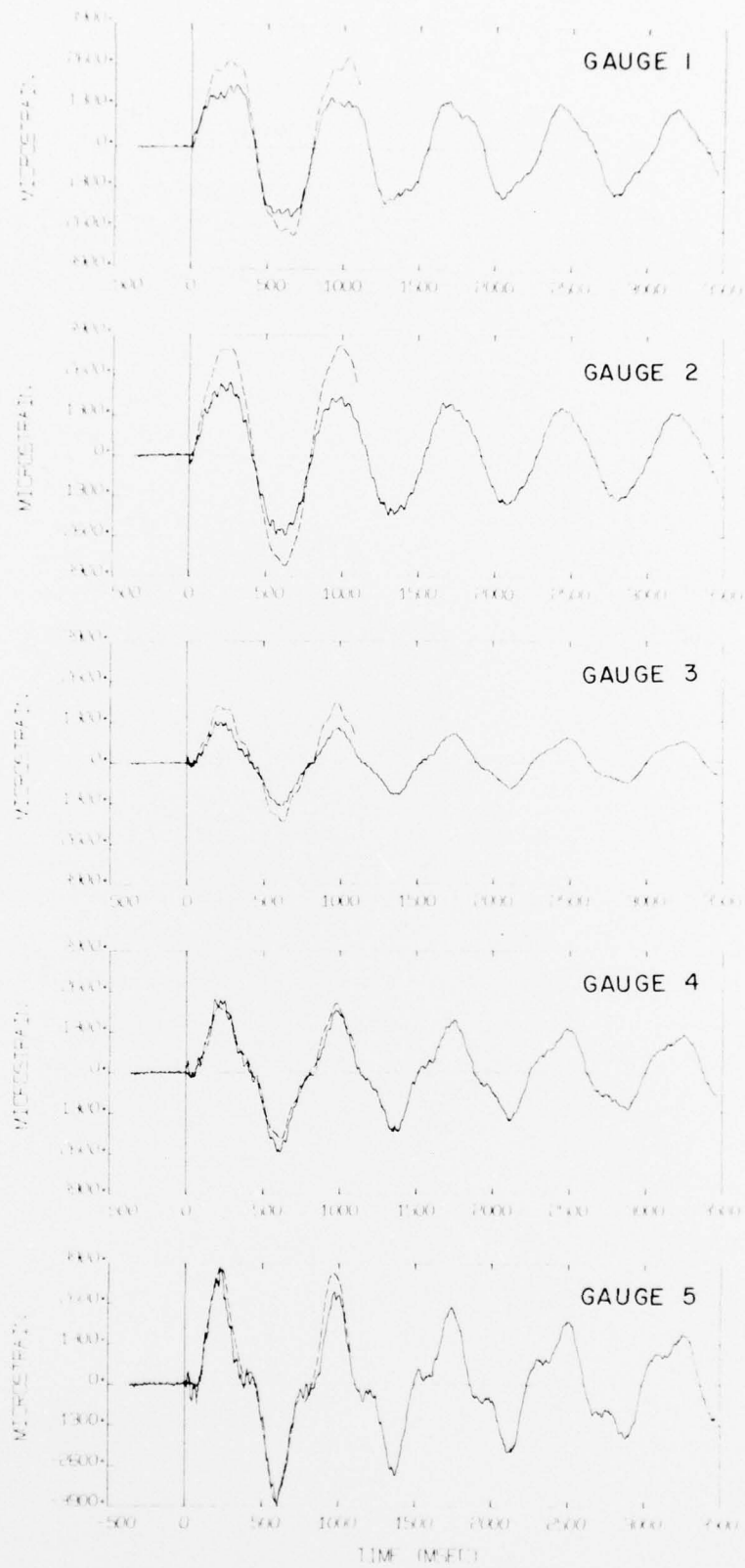


FIG. 15 COMPARISON OF BENDING STRAIN PREDICTIONS SET 4 (DASHED LINES) AGAINST THE MEASURED STRAINS (SOLID LINES) FOR THE 7.0 PSI WHIP ANTENNA AT GAUGE LOCATIONS 1 TO 5.

UNCLASSIFIED

UNCLASSIFIED

STP 448

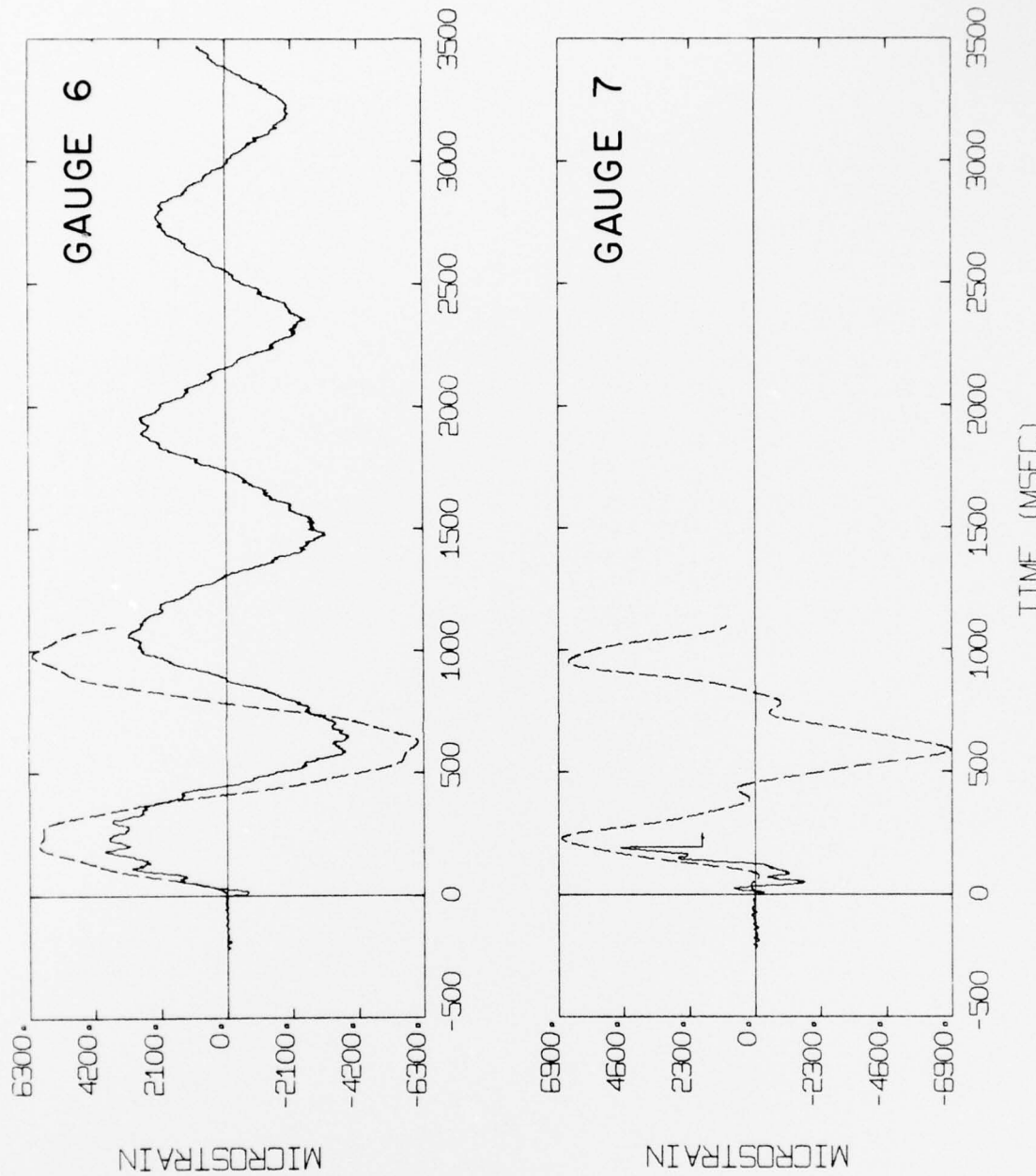


FIG. 16 COMPARISON OF BENDING STRAIN PREDICTIONS SET 4 (DASHED LINES) AGAINST THE MEASURED STRAINS (SOLID LINES) FOR THE 10.0 PSI WHIP ANTENNA AT GAUGE LOCATIONS 6 AND 7.

UNCLASSIFIED

UNCLASSIFIED

STP 448

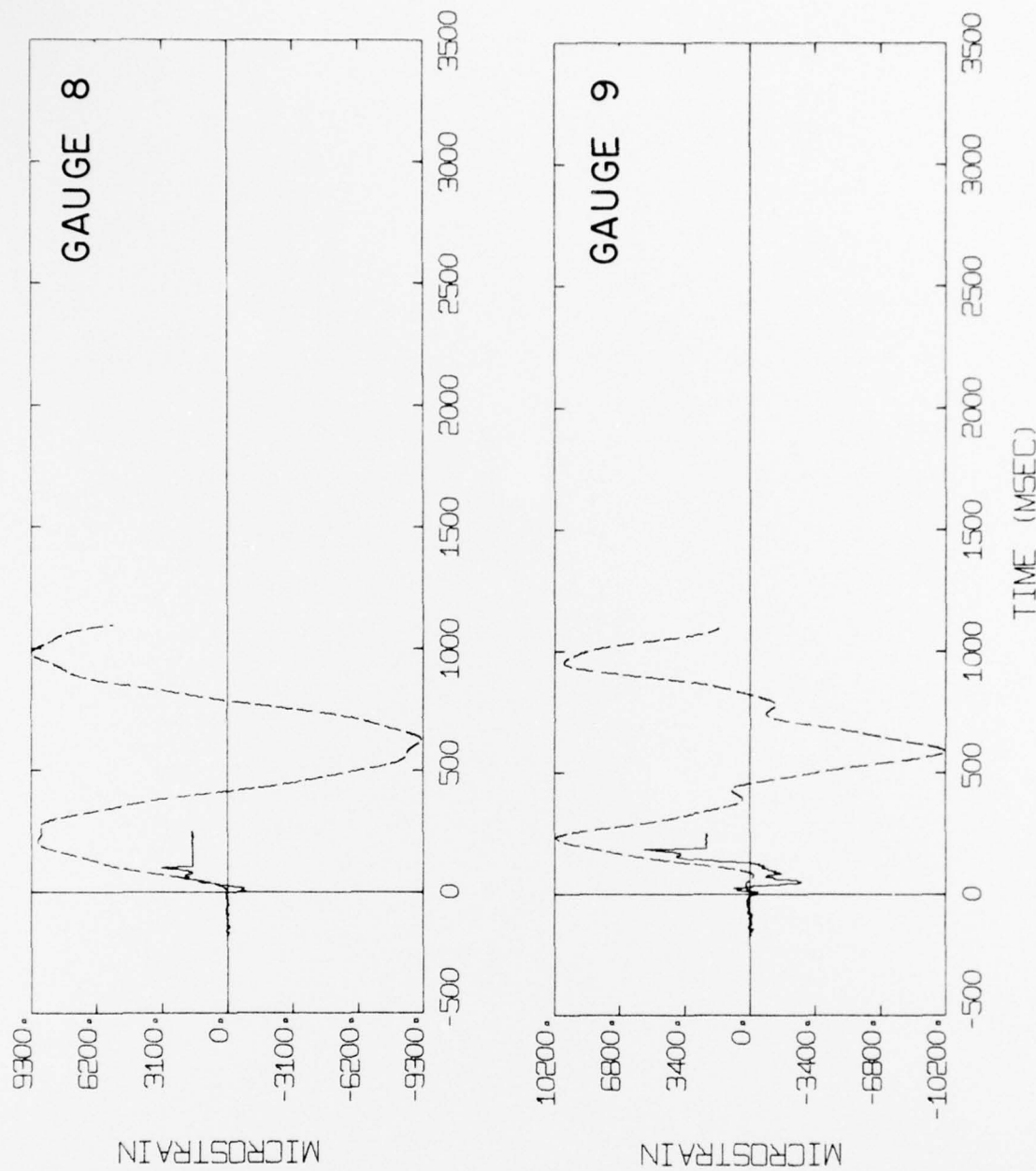


FIG. 17 COMPARISON OF BENDING STRAIN PREDICTIONS SET 4 (DASHED LINES) AGAINST THE MEASURED STRAINS (SOLID LINES) FOR THE 10.0 PSI WHIP ANTENNA AT GAUGE LOCATIONS 8 and 9.

UNCLASSIFIED

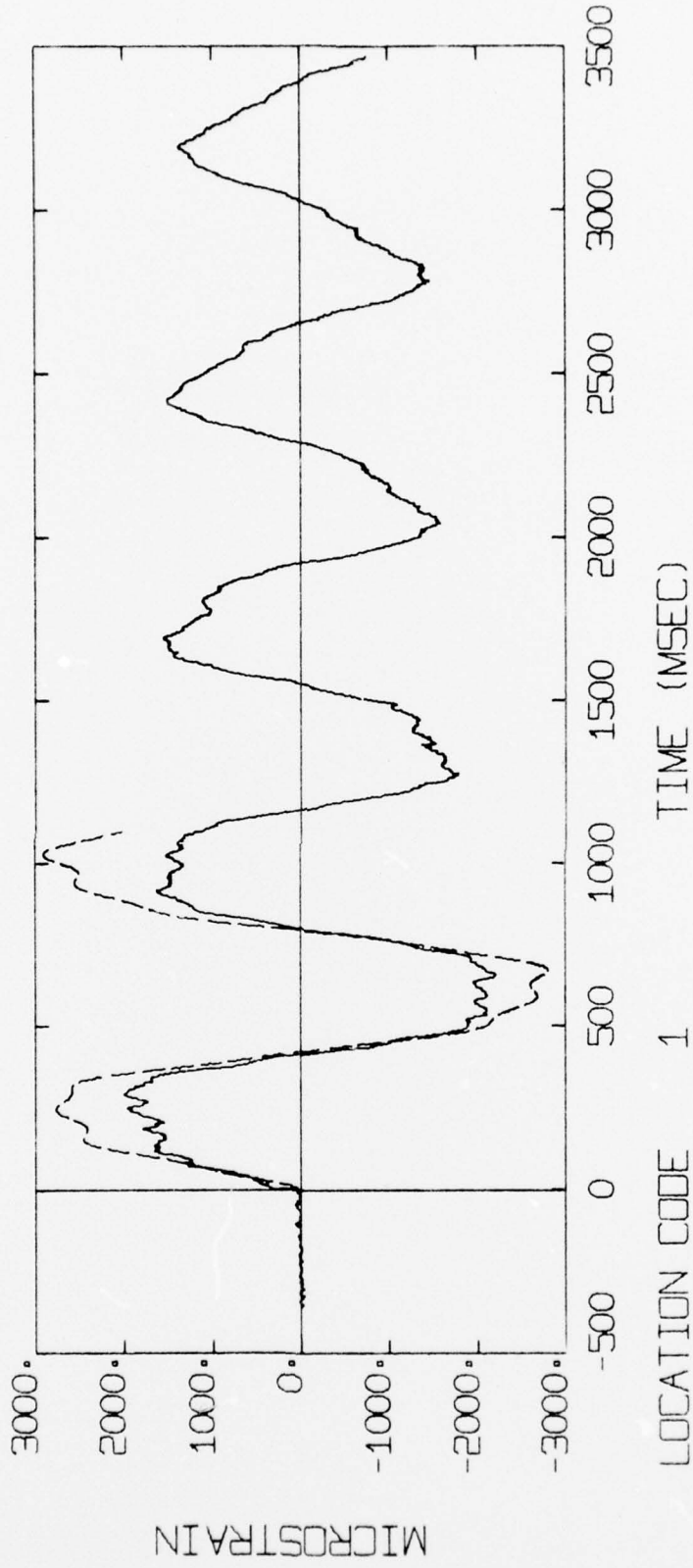


FIG. 18 COMPARISON OF BENDING STRAIN PREDICTIONS SET 4 (DASHED LINES) AGAINST THE MEASURED STRAINS (SOLID LINES) FOR THE 7.0 PSI WHIP ANTENNA AT GAUGE LOCATION 1.

UNCLASSIFIED

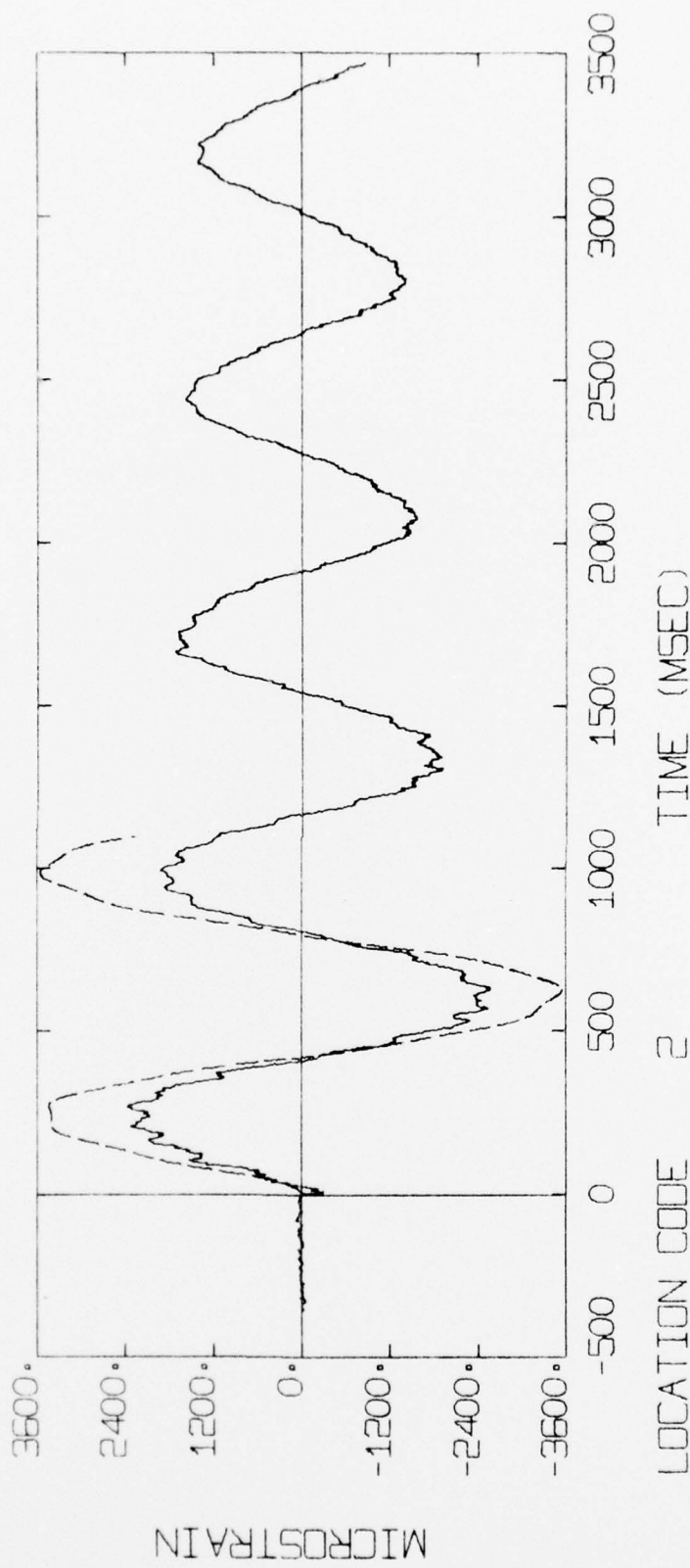


FIG. 19 COMPARISON OF BENDING STRAIN PREDICTIONS SET 4 (DASHED LINES) AGAINST THE MEASURED STRAINS (SOLID LINES) FOR THE 7.0 PSI WHIP ANTENNA AT GAUGE LOCATION 2.

UNCLASSIFIED

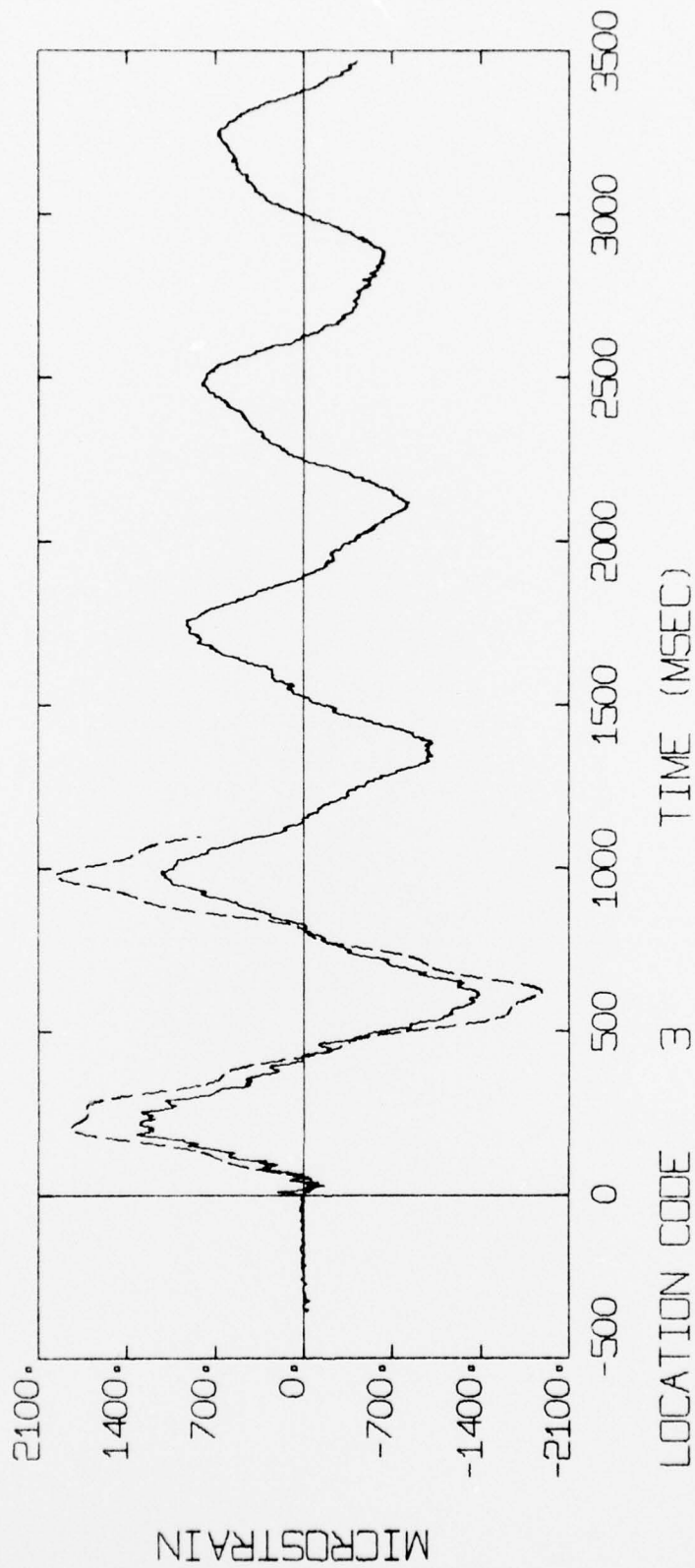


FIG. 20 COMPARISON OF BENDING STRAIN PREDICTIONS SET 4 (DASHED LINES) AGAINST THE MEASURED STRAINS (SOLID LINES) FOR THE 7.0 PSI WHIP ANTENNA AT GAUGE LOCATION 3.

UNCLASSIFIED

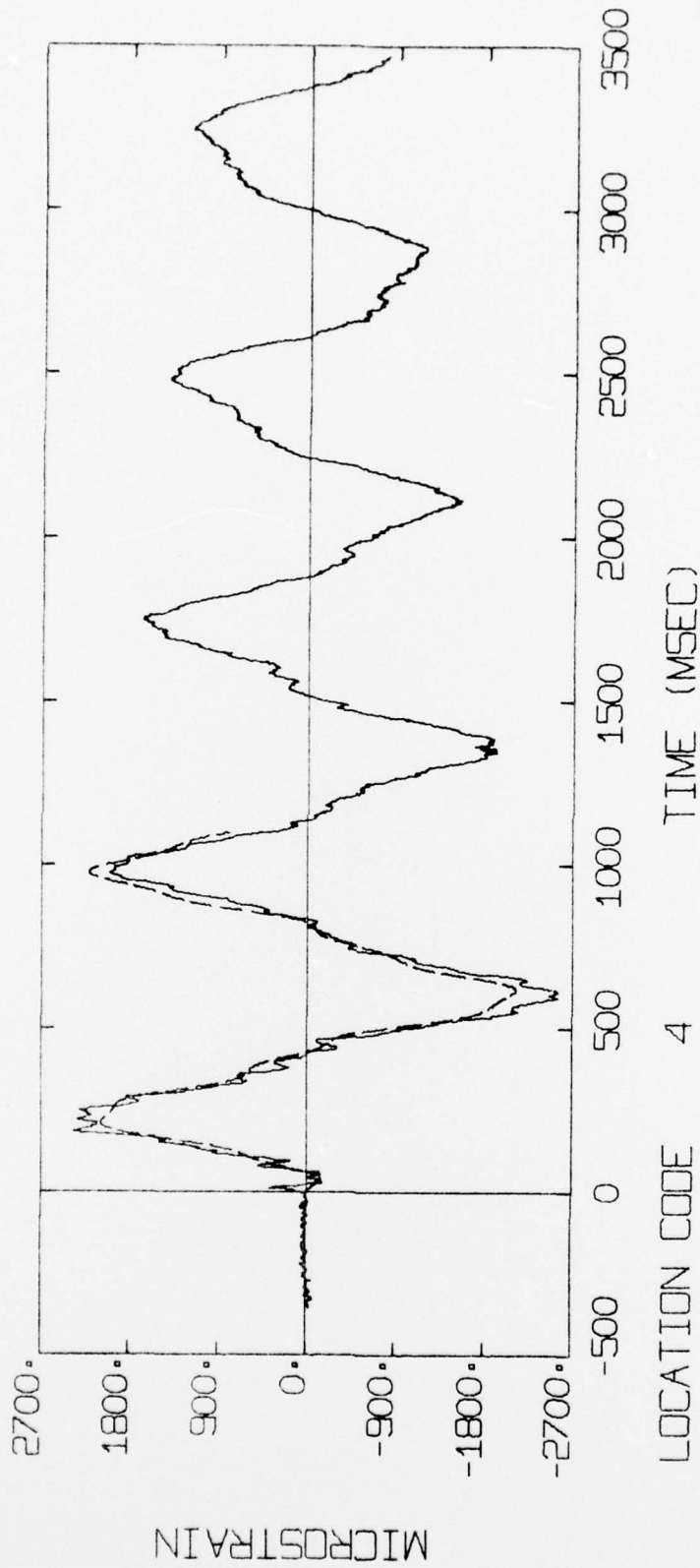


FIG. 21 COMPARISON OF BENDING STRAIN PREDICTIONS SET 4 (DASHED LINES) AGAINST THE MEASURED STRAINS (SOLID LINES) FOR THE 7.0 PSI WHIP ANTENNA AT GAUGE LOCATION 4.

UNCLASSIFIED

UNCLASSIFIED

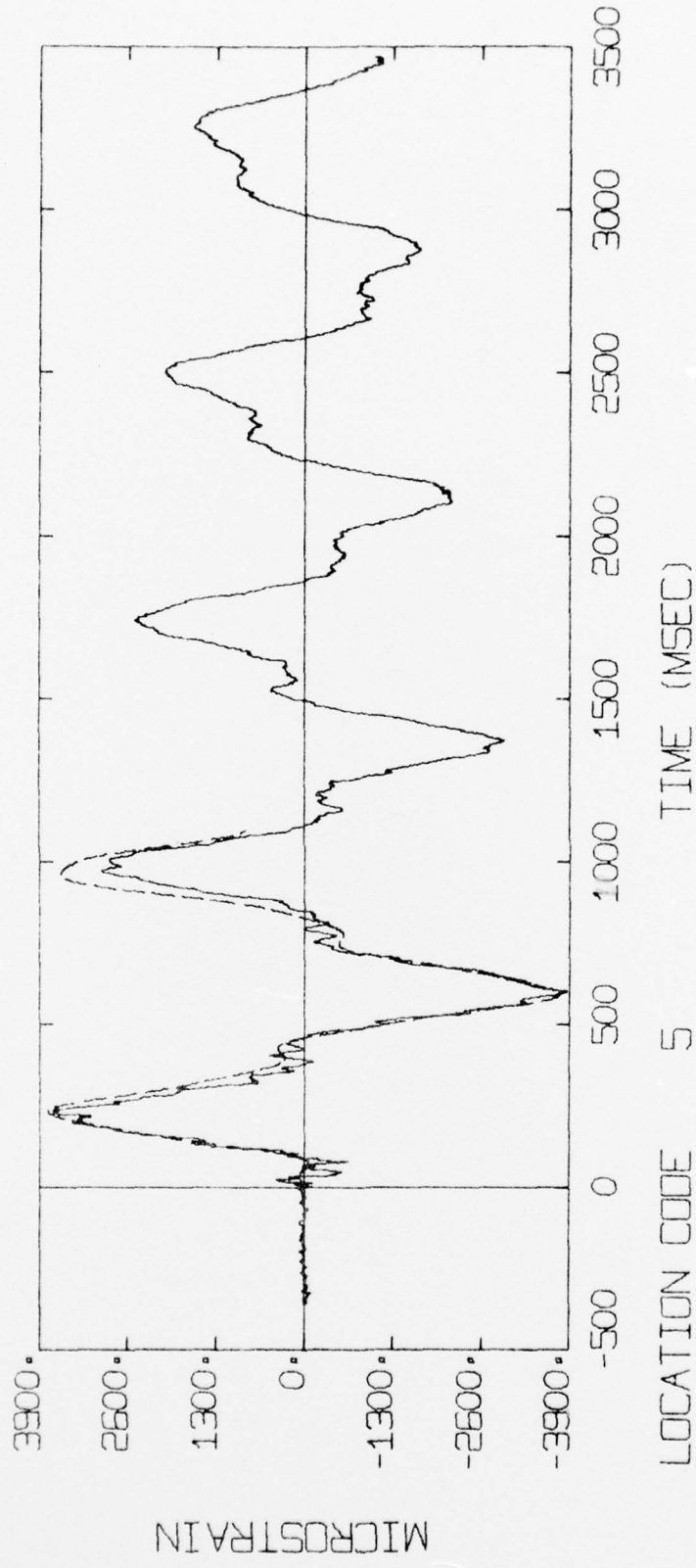


FIG. 22 COMPARISON OF BENDING STRAIN PREDICTIONS SET 4 (DASHED LINES) AGAINST THE MEASURED STRAINS (SOLID LINES) FOR THE 7.0 PSI WHIP ANTENNA AT GAUGE LOCATION 5.

UNCLASSIFIED

UNCLASSIFIED

Security Classification

DOCUMENT CONTROL DATA - R & D

(Security classification of title, body of abstract and indexing annotation must be entered when the overall document is classified)

1. ORIGINATING ACTIVITY Defence Research Establishment Suffield		2a. DOCUMENT SECURITY CLASSIFICATION UNCLASSIFIED
		2b. GROUP
3. DOCUMENT TITLE BLAST RESPONSE OF 35 FT FIBREGLASS WHIP ANTENNA - EVENT DICE THROW (U)		
4. DESCRIPTIVE NOTES (Type of report and inclusive dates) Technical Paper		
5. AUTHOR(S) (Last name, first name, middle initial) Price, G.V. and Coffey, C.G.		
6. DOCUMENT DATE November 1977	7a. TOTAL NO. OF PAGES 43	7b. NO. OF REFS 8
8a. PROJECT OR GRANT NO. PROJECT NO. 97-80-01	9a. ORIGINATOR'S DOCUMENT NUMBER(S) Suffield Technical Paper No. 448	
8b. CONTRACT NO.	9b. OTHER DOCUMENT NO.(S) (Any other numbers that may be assigned this document)	
10. DISTRIBUTION STATEMENT UNLIMITED DISTRIBUTION		
11. SUPPLEMENTARY NOTES	12. SPONSORING ACTIVITY	
13. ABSTRACT The blast response of 35 ft fibreglass Whip Antennas was investigated in a free-field blast trial and in numerical simulation experiments. The antennas satisfactorily withstood the air blast loading at nominal 7.0, 10.0 and 12.2 psi peak overpressure locations in Event Dice Throw. The numerical model predictions for the natural frequencies are in excellent agreement with results obtained experimentally, however the corresponding predictions for the transient strain using drag coefficients based on previous trials were approximately double the values obtained experimentally. Subsequent revised numerical predictions for the transient strains using experimental drag coefficients obtained independently in the blast trial itself have produced results in more reasonable agreement with the experimental transient strains.		
(U)		

UNCLASSIFIED

Security Classification

KEY WORDS

Dice Throw
Antenna Studies
Blast response
Numerical simulation

INSTRUCTIONS

1. ORIGINATING ACTIVITY: Enter the name and address of the organization issuing the document.
- 2a. DOCUMENT SECURITY CLASSIFICATION: Enter the overall security classification of the document including special warning terms whenever applicable.
- 2b. GROUP: Enter security reclassification group number. The three groups are defined in Appendix 'M' of the DRB Security Regulations.
3. DOCUMENT TITLE: Enter the complete document title in all capital letters. Titles in all cases should be unclassified. If a sufficiently descriptive title cannot be selected without classification, show title classification with the usual one-capital-letter abbreviation in parentheses immediately following the title.
4. DESCRIPTIVE NOTES: Enter the category of document, e.g. technical report, technical note or technical letter. If appropriate, enter the type of document, e.g. interim, progress, summary, annual or final. Give the inclusive dates when a specific reporting period is covered.
5. AUTHOR(S): Enter the name(s) of author(s) as shown on or in the document. Enter last name, first name, middle initial. If military, show rank. The name of the principal author is an absolute minimum requirement.
6. DOCUMENT DATE: Enter the date (month, year) of establishment approval for publication of the document.
- 7a. TOTAL NUMBER OF PAGES: The total page count should follow normal pagination procedures, i.e., enter the number of pages containing information.
- 7b. NUMBER OF REFERENCES: Enter the total number of references cited in the document.
- 8a. PROJECT OR GRANT NUMBER: If appropriate, enter the applicable research and development project or grant number under which the document was written.
- 8b. CONTRACT NUMBER: If appropriate, enter the applicable number under which the document was written.
- 9a. ORIGINATOR'S DOCUMENT NUMBER(S): Enter the official document number by which the document will be identified and controlled by the originating activity. This number must be unique to this document.
- 9b. OTHER DOCUMENT NUMBER(S): If the document has been assigned any other document numbers (either by the originator or by the sponsor), also enter this number(s).
10. DISTRIBUTION STATEMENT: Enter any limitations on further dissemination of the document, other than those imposed by security classification, using standard statements such as:
 - (1) "Qualified requesters may obtain copies of this document from their defence documentation center."
 - (2) "Announcement and dissemination of this document is not authorized without prior approval from originating activity."
11. SUPPLEMENTARY NOTES: Use for additional explanatory notes.
12. SPONSORING ACTIVITY: Enter the name of the departmental project office or laboratory sponsoring the research and development. Include address.
13. ABSTRACT: Enter an abstract giving a brief and factual summary of the document, even though it may also appear elsewhere in the body of the document itself. It is highly desirable that the abstract of classified documents be unclassified. Each paragraph of the abstract shall end with an indication of the security classification of the information in the paragraph (unless the document itself is unclassified) represented as (TS), (S), (C), (R), or (U).
The length of the abstract should be limited to 20 single-spaced standard typewritten lines; 7½ inches long.
14. KEY WORDS: Key words are technically meaningful terms or short phrases that characterize a document and could be helpful in cataloging the document. Key words should be selected so that no security classification is required. Identifiers, such as equipment model designation, trade name, military project code name, geographic location, may be used as key words but will be followed by an indication of technical context.